C.P. No. 1251

PROCUREMENT EXECUTIVE, MINISTRY OF DEFENCE

AERONAUTICAL RESEARCH COUNCIL

CURRENT PAPERS

The Effect of Leading-Edge Geometry on High-Speed Stalling

by

G. F. Moss, R.A.E , Farnborough

A. B. Haines and R Jordan, A.R.A., Bedford

LONDON: HER MAJESTY'S STATIONERY OFFICE

1973

PRICE *90p* NET

UDC 533.691.1 : 533.6.013.66 : 533.6.013.13 : 533.694.26 : 533.691.13

CP No.1251*
May 1972

THE EFFECT OF LEADING-EDGE GEOMETRY ON HIGH-SPEED STALLING

by

G. F. Moss, RAE, Farnborough
A. B. Haines, ARA, Bedford
R. Jordan, ARA, Bedford

SUMMARY

In the first part of this paper it is shown by means of an example how small modifications to the leading-edge profile of a sweptwing can result in large effects on lift performance at the stall in the higher range of subsonic speeds. The basic types of leading-edge pressure distribution for any one fixed geometry over the whole range of subsonic speed are discussed and the difficulties in designing a profile shape which gives a satisfactory compromise in wing performance across this range is emphasized.

In the second part of the paper, two types of variable-geometry device at the leading edge are discussed, each of which allows some degree of optimization in the shape required for good aerodynamic performance across the range of Mach number. The first of these, the leading-edge slat, is shown to work in quite a different way at high speeds from that in its more conventional role at landing and take-off conditions. Recent UK research work is used to demonstrate some important aerodynamic features of slats when used at high speeds in near-optimum positions. The second type of variable-geometry device is a new one, recently developed within the UK. The essential feature is a linkage system, entirely contained within the nose of the profile, which can be used to change the shape of the leading edge of the 'clean' wing in such a way to improve performance over a range of aerodynamic conditions. The aerodynamic possibilities of the use of this device in the higher subsonic speed range are demonstrated by reference to some recent UK wind-tunnel tests.

This Report gives the written version of a lecture prepared for presentation at the AGARD Specialists' Meeting, "Fluid Dynamics of Aircraft Stalling", Lisbon, April 1972

---

* Replaces RAE Technical Report 72099 - ARC 34097

CONTENTS

1 INTRODUCTION

In the design of sweptwings one of the choices which has to be made at an early stage is the selection of the wing-section profile shape (or shapes) to be used. This selection is made very often with the help of theoretical work and two-dimensional wind-tunnel tests, having due regard to the operational requirements of the project throughout the speed range and to the various constraints imposed by structural considerations. The design requirements are usually in conflict and as a result the final choice of profile to be used is generally a 'best compromise' which can have serious deficiencies at one or more important points in the flight envelope. Considering the design of the profile at the leading edge, variable-geometry in the form of slats, Kruger flaps or other such devices is generally found essential to meet the particular deficiency which arises at low-speed, high-lift conditions (for take-off and landing), and recently the use of these devices set at intermediate angles has been resorted to in order to improve stalling characteristics at high subsonic speeds (for high-speed manoeuvres). But a high price is paid for the use of leading-edge devices at high-speeds. The higher loading conditions imply extra weight to be carried and the need to specify precisely extra settings implies complications to the structure and control system. Also some of the aerodynamic effects can be adverse. Because of the extra drag involved for instance, performance at 'cruise' can be sacrificed in some important respects.

Two points therefore need to be stressed at the start of this discussion. Firstly, it is important to increase our understanding of the particular sensitivities of stalling characteristics at high speeds to small variations in leading-edge profile shape, and secondly it is necessary to be more aware of the aerodynamic situations which arise when devices such as leading-edge slats are used to improve maximum-usable-lift at high subsonic speeds. It is hoped that this Report will contribute a little on both these issues.

1.1 Basic types of pressure distribution at the leading edge

In the higher-subsonic speed range, the stall of sweptwings is primarily associated with the development of flow separations due to the interaction of the shock wave system on the upper-surface of the wing with the boundary-layer. The situations which arise at flow separation can be extremely complex even in two-dimensional flow, particularly when there is interaction between these shock induced separations and separations near the trailing-edge[1]. On the

complete sweptwing the flow fields are affected by root and tip effects and the interference from the body, the nacelles and stores (if any). With increase of Mach number these three-dimensional effects are aggravated as the effective aspect ratio is reduced. However, provided the leading-edge sweep is not excessive and the leading-edge radius is not so small that leading-edge separations of the slender-wing type develop, a viable approach to the problems of separation can be made by considering the flows as quasi-two-dimensional in the first instance, taking account of the three-dimensional implications subsequently.

Thus we may start by considering three main types of upper-surface pressure distribution near the leading edge, which can occur at conditions just prior to flow breakdown on a particular aerofoil (Fig.1). Three examples are shown with approximately the same shock strength. At the lower end of the high subsonic range under discussion, say at speeds near M = 0.5, the flow usually separates at the shock which is very close to the leading edge and which increases in strength as lift is increased. At higher speeds, however, a nearly constant velocity supercritical region tends to develop over the forward part of the wing upper-surface, terminating in a shock wave which moves further aft and increases in strength with increased lift until the separation of the flow from the surface is induced. At still higher speeds the supercritical region may extend as far back as 55%-65% of the wing chord and the shock, when strong enough to cause separation, is typically preceded by a progressive increase in local velocity. In all these phases of development, each culminating in the stall, the geometry of the leading edge plays a critical part, either directly because of local effects on the shock waves, or indirectly because of effects on the general state of the boundary-layer and thus on its tendency to separate further aft on the wing upper surface. Bearing these three main types of leading-edge pressure distribution in mind, three specific examples of leading-edge geometry changes will be presented and discussed in this paper.

1.2 Specific examples of leading-edge geometry changes

Using the first of these examples, described below in section 2, it is shown how a small modification to the leading-edge profile can cause large effects on lift performance which are only beneficial at one end of the high subsonic speed range. The need for a satisfactory compromise across the whole range is thus emphasized. In the second example given in section 3, the use of leading-edge slats at high subsonic speeds is discussed and by reference to

some recent UK research studies these devices are shown to work in quite a different way from their more conventional use at low speeds. Finally, section 4 describes the use of a new type of variable-geometry device, recently developed within the UK. The use of this device to improve lift performance across the whole of the high subsonic speed range will again be demonstrated by reference to some recent UK test data.

2 WING-SECTION PROFILE CHANGES

The first piece of work presented concerns a modification made to the leading-edge profile of a variable-sweep research model. Details of the complete model configuration used in the investigation are given in Fig.2. Two sweep angles for the wings were used in the investigation and the appropriate values of aspect-ratio and wing-twist ('wash-out') are noted on the Figure. One model was used for the measurement of forces (presented in Figs.7 and 8) and another rather larger version of the same configuration was used for the measurement of pressure data, (quoted in Figs.9 and 10). The wing-section employed is also shown in Fig.2, designated as 'basic wing-section 'A''. Two-dimensional tunnel data for this section and for the modified section 'B' is quoted in Figs.1 and 3-6.

2.1 Two-dimensional considerations

The basic section 'A' used on this model was a comparatively thick one (about 13% thick, perpendicular to the wing quarter-chord line) and had a reasonable degree of rear loading and a fairly small leading-edge radius.

Fig.3 shows the stall boundary obtained for this profile as obtained from two-dimensional tests and the criteria used to define this boundary are also indicated by means of inset sketches in the Figure. The three types of pressure distribution shown in Fig.1 have been taken from this same set of test data. As will be seen the boundary is fairly flat from $M = 0.4$ up to $M = 0.58$ and over this range of Mach number we have the first type of pressure distribution mentioned previously with a very sharp suction peak and a strong shock near the leading edge at conditions before flow breakdown. In the region $0.6 < M < 0.65$, however the second type of pressure distribution applies, with a nearly-constant-velocity supercritical region developing over the forward part of the profile upper-surface terminating in a strong shock. At higher Mach numbers, the third type of distribution shown in Fig.1 is apparent, velocities building steadily from the leading edge to form a triangular type of supercritical distribution culminating in a strong shock much further back on the chord. Fig.3 also includes a sketch showing in what manner the leading-edge

profile was modified to form the second profile designated as wing section 'B'. The modifications of most significance were the increase in nose droop and the change to the local surface curvature round the leading edge. The effect on the sectional stall boundary is given also in Fig.3 and shows that the maximum lift of the profile has been raised at the low end of the speed range without apparent harm to the performance at the higher Mach numbers. The marginal improvement at high speeds is possibly due in part to the small change in section thickness (about 0.3%) also included in the modification, so no credit can really be taken for this. It is of course all too easy to modify the leading-edge shape of a profile to improve the maximum lift developed at low speeds at the expense of performance at the high end of the range, so this particular modification very much represents a compromise solution. Also, as anyone acquainted with so-called 'supercritical' types of aerofoils will know, it is all too easy (but not necessarily inevitable) to devise sections with substantial improvements in maximum lift at high speeds at the expense of usable lift at low speeds. Before leaving this figure attention must be drawn to the scale of equivalent Mach number included for the wings of the complete model when set at 27.2° sweep. As will be seen the benefits of the sectional modification reduce with increasing Mach number becoming virtually zero at a Mach number of about 0.7 for the wing at this sweep setting. For the wing swept at 42.2°, this Mach number would be in the region of $M = 0.85$.

Before discussing the actual effects of this sectional modification on the measured lift coefficients for the complete sweptwing, it is worth considering briefly how these benefits in lift coefficient have materialized. Fig.4 shows the lift-incidence curve for both the basic section 'A' and the modified section 'B' at $M = 0.5$. There is a change in the lift developed at constant incidence before the stall, mainly due to the change in overall chordwise camber, but of more significance is the increase in the maximum lift developed. From the measured pressure data there is evidence of a reduction in suction-peak height, and thus a reduction in shock strength, for the same lift at conditions prior to flow breakdown (a comparison at $C_L = 1.14$ is shown to demonstrate this in the inset diagram). Since the maximum lift attained is by and large governed by the strength of the shock reaching some critical value, the result is an overall increase in maximum lift-coefficient in favour of the modified section (0.09 at this Mach number). At high Mach numbers a different flow situation arises and it is instructive to consider in this case the comparison of pressure distribution at high lift when the shock terminating the supercritical region on the two profiles is likely to have the same effect on the boundary-layer behaviour. Fig.5 shows what the comparison between the

lift-incidence curves looks like for the two sections at M = 0.7, and the inset diagram shows the comparison of upper-surface pressure distribution at an incidence of about 3.5° when the shock has about the same strength and position on the chord. Marginal benefits to usable lift at this Mach number partly arise from the section modification due to increased suctions being induced aft of the leading edge in the supercritical region.

Fig.6 demonstrates some extra important effects of this section modification in two-dimensional conditions. Firstly, there was a general tendency for the upper-surface shock on the modified section to be a little further aft when compared on a C_L basis, (except at M = 0.66). Secondly, the forward movement of the shock as flow separations developed tended to be more abrupt on the modified section. As may be seen from the typical pressure distribution in Fig.5, the more triangular form of the supercritical pressure distribution on the original section would tend to make the shock weaker as it moved forward. The resultant stabilizing effect on the stall development would not have been present on the modified section with its much flatter supercritical pressure distribution ahead of the shock. Thirdly, at the higher Mach numbers, the shock strength as compared on a C_L basis tends to be weaker on the modified section at conditions before the onset of flow separations. However, as flow separations develop, the shock grows in strength much more rapidly and this trend is reversed (case for M = 0.7 is shown). We shall refer to these points later in the discussion.

2.2 Application to the complete model configuration

Turning now to the lift-coefficients measured on the complete model of Fig.2 before and after this leading-edge modification was incorporated, we see that the promise of improvement from the two-dimensional tests has not entirely been fulfilled. In Fig.7a the lift-incidence curves for the configuration with wings set at 27.2° sweep are shown. Whereas the leading-edge modification has improved the maximum lift at the lower Mach numbers, at the higher speeds positive harm is done, the C_{Lmax} being lower and early breaks appearing in the curves. The benefits at lower speeds reduce to zero by M = 0.70 and it is interesting that this at least was predicted from two-dimensional tests (equivalent M = 0.63). Before discussing the reasons for the losses in maximum lift at the higher speeds, it is instructive to note some similarities with the lift-incidence characteristics measured at the higher wing sweep of 42.2° (Fig.7b). The benefits of the modification made to the wing leading edge are not so marked at the lower Mach numbers even allowing for the normal sweep effect, and there are indications in the more gradual nature of

the loss of lift at high incidence that the stall is altogether more three-dimensional in character than at the lower sweep. However, there is once more a tendency for these benefits at low speed to disappear at about M = 0.85, i.e. at virtually the same equivalent two-dimensional Mach number found at the lower wing sweep, M = 0.65. At the higher Mach numbers, i.e. above M = 0.70 at the lower wing sweep and M = 0.85 at the higher wing sweep, an early break develops in the lift curves when the modified section is used, due to premature flow separations outboard on the wing. Thus the value of usable lift has been made worse rather than left unchanged as demonstrated in the two-dimensional data (Fig.3). Taken as a whole we would say that the leading-edge modification made to the basic wing section, although restricted in the improvement achieved at low speeds in order to maintain performance at the higher speeds, has only shown benefits up to M = 0.70 at the wing sweep of 27.2° and up to M = 0.85 at the wing sweep of 42.2°. Above these points in the subsonic speed range positive harm has been done to the stall boundary.

The reasons for this state of affairs at the higher Mach numbers is explained by reference to some pressure measurements made on the complete model. Fig.8 shows for a Mach number of 0.80 with the wings swept 27.2° the development of the local chordwise lift-coefficient at two spanwise stations as incidence is increased. A comparison is shown with the equivalent two-dimensional data, due allowance having been made for induced incidence and body-upwash increments at each position. The figure shows how at 60% semi-span the development of local lift is at least as great as, if not greater than, the sectional characteristic, but at stations nearer the tip there is an early break, ($\alpha = 2\frac{1}{2}^{\circ}$), in the development of life resulting in significant losses over this region of the wing at the final stall boundary ($\alpha = 7^{\circ}$, see Fig.7a). At inboard chordwise stations (not shown) very much better lift-incidence characteristics than those found in two-dimensions are developed and the general picture which emerges at these higher subsonic speeds is of strong three-dimensional effects on the spanwise loading and on the character of the flow development up to the stall, biased against good performance at the tip. It is worth noting from this figure that the order of wing twist needed to postpone flow separation at the tip is large, even were this permissible from other (aerodynamic) considerations.

It is useful to look at the chordwise pressure distribution at these two spanwise stations, and this has been done in Fig.9 for those points in the lift development indicated by the 'diamond' symbols marked in Fig.8. Comparison is made with the equivalent two-dimensional pressure distributions marked similarly

by 'circle' symbols. For each spanwise station the comparison is made at about the same lift-coefficient and in each case the conditions taken are those just before the break in the local lift development with incidence (in either the two-dimensional or the three-dimensional data). This comparison shows, that although agreement in the pressure distribution at 60% semispan is fairly good, at 90% semispan the shock terminating the supercritical region is both stronger and further forward on the complete model and that there is a tendency for increased suctions to develop over the forward portion of the supercritical region resulting in a higher, flatter roof-top type pressure distribution. These observations are entirely compatible with the classic situation which arises on straight-tapered sweptwings of constant chordwise section[2,3]. At the tip, thickness effects cause local reductions in isobar sweep, towards the leading edge, and a little further inboard, (say at 2/3 to 3/4 semispan), a maximum in the spanwise loading gives rise to comparatively higher local lift-coefficients. Taken together these two factors induce a shock front at high-subsonic speeds which is of reduced sweep over the whole outer portion of the wing upper-surface and shocks which are thus further forward and of higher strength than elsewhere on the wing. The result is that shock-induced separations generally occur first near the tip and progress inboard as incidence is increased.

Thus we may obtain some insight into why the leading-edge modification applied to the basic wing section did harm on the complete model in the higher range of speeds. The situation is summarized in Fig.10. In the lower half of the diagram attention is drawn to the classic three-dimensional effects on shock position, and in the upper half the effects of the section modification are shown. At mid-span, at near-two-dimensional conditions, we can see that the expected increase in suction at the forward end of the supercritical region due to the modification, (see Fig.5), can easily be accommodated with some benefit and the tendency for a further aft shock (see Fig.6) will do little harm locally and even some good. However, this further aft position of the shock locally at mid-span indirectly has an adverse effect because it makes worse the basic tendency for the shock to become less swept over the outer portions of the wing. At the wing tip adverse effects are more obvious. The increase of suction forward on the profile will in this case cause adverse pressure gradients to appear in the supercritical region resulting in the shock moving forward more abruptly at an earlier incidence and becoming stronger as it does so. Thus the section modification will have aggravated the classic

development of shock-induced flow separations usual on sweptwings by a tendency to reduce shock sweep and increase shock strength over the whole of the outer wing. The features which bring this about are apparent in the sectional characteristics but do no harm in two-dimensional conditions. It should be noted that at low speeds in the range of Mach number under review, shock inducing flow separations only occur at positions very close to the leading edge so none of this argument about shock movements applies. The wing in three-dimensions can thus take advantage of the gains demonstrated in the sectional test data at these speeds.

2.3 The need for variable geometry

The foregoing discussion centred round the measured effects of a particular modification to the leading-edge shape of a profile used on a sweptwing at high subsonic speeds leads to two conclusions. Firstly, the requirements at the low and high ends of the high-subsonic speed range are basically in conflict as regards the improvement of usable lift. At lower speeds the strong adverse gradient and/or shock strengths which develop at high incidences can be reduced by the use of leading-edge nose-down camber, although in excess this can lead to subsidiary problems at other flight conditions. However, at the high end of this speed range, application of this nose camber can increase velocity, and thus the local shock strengths, at critical conditions. Secondly, even when great care is taken not to compromise the performance of the wing section at high speeds by modifications made to improve the performance at the lower speeds, - and this can be first well established by two-dimensional tests - basic three dimensional effects on the complete wing at the higher speeds can result in strong adverse effects at the stall due to such modifications.

The case for variable geometry rests on the basic need to resolve the conflicting requirements of leading-edge geometry across the high-subsonic speed range. In the last section of this paper the possible use of variable leading-edge profiles is presented as a means to improve performance over a wide range of speed, but first the aerodynamics of leading-edge slats at high speeds is discussed below.

3 THE USE OF LEADING-EDGE SLATS AT HIGH SUBSONIC SPEEDS

At moderate subsonic speeds such as $M = 0.5$, when the shockwave is near the leading edge, the mechanism by which a leading-edge slat can give an increase in usable C_L is essentially the same as at low speeds. Deflection

and extension of the slat can reduce the peak suction near the leading edge and, so delay the onset of a shock-induced separation. Typically, the optimum deflection is roughly half that used for landing. At higher subsonic speeds, however, e.g. M = 0.65 for 25° sweep or M = 0.80 for 45° sweep, a slat can still improve the stalling characteristics but the nature of the improvement and the mechanism by which it is achieved are not the same as at lower speeds. A fair amount of research has been undertaken within the UK during the past four years to show what factors then contribute to a good slat design for wings of similar thickness to those discussed earlier and how to retain the effectiveness up to as high a Mach number as possible.

Initially, tests were made on a high aspect ratio wing with 27° leading-edge sweepback (not the same wing as that discussed earlier but of similar thickness) with three slat designs A, B, C (Fig.11) and one droop design B formed by fairing over the slot of slat B. The leading-edge devices extend over the full span of the nett wing but because the wing design includes three-dimensional treatment with the section shape varying across the span, the slot geometry also varies considerably as shown in Fig.11. Overall $C_L - \alpha$ curves are shown in Fig.12 for M = 0.55 and 0.65 and typical pressure distributions over the forward part of the wing at mid-semi-span at M = 0.65 are compared in Figs.13a and b. It will be seen that at M = 0.55, slat A which is drooped 12.5° over most of the span improves the maximum lift by at least $\Delta C_L = 0.2$ but it is the results for M = 0.65 that are of more interest and which pose the greater challenge. The first point to note is that the high-lift performance of the clean wing is particularly good at M = 0.65, the maximum usable lift being assessed as $C_L = 1.04$ as compared with $C_L = 0.84$ at M = 0.55 or $C_L = 0.89$ at M = 0.71. Pressure-plotting tests showed that a high lift at M = 0.65, the local supersonic region over the forward upper surface of the clean wing was well-conditioned with a peak suction near the leading edge followed by a largely isentropic recompression back to a relatively weak shock. It was therefore realised from the outset that it might be difficult to obtain sizeable improvements through the use of high-lift devices and at first sight the results in Fig.12 do not appear too encouraging. Slat A is clearly deflected too much and gives a reduction of at least 0.15 in usable maximum lift-coefficient, irrespective of how this is defined. Slats B and C are more difficult to assess: pessimistically, the break in the $C_L - \alpha$ curve again occurs at a lower C_L than for the clean wing but with slat C at least, the ultimate $C_{L_{max}}$ is higher. It is only droop B that gives a clear improvement, by about $\Delta C_L = 0.09$ of which

only 0.03 can be ascribed to the extra wing area. Referring to the pressure distributions in Fig.13, it will be seen that at moderate incidences, e.g. $\alpha = 8.7^{\circ}$ in Fig.13a, droop B produces two local supersonic regions, the first near the leading edge and the second near 0.10c but at higher incidences, e.g. $\alpha = 10.9^{\circ}$ and 13.1°, these link to give an extensive peaky supersonic region with considerable isentropic recompression ahead of the shock. The results with droop B are therefore similar in character to those for the clean wing but higher values of C_L for separation-onset are achieved because the supersonic region as can be imagined, is more extensive. One should note however that no results are presented for droop B beyond $\alpha = 13.1^{\circ}$. This is because severe model bounce developed and it was impossible to obtain any steady readings. To judge from experience on other models, the likely explanation is that the shockwave moved forward rapidly and the supersonic region round the leading edge failed to develop over part of the span. This means that high values of C_L for separation-onset had been achieved at the expense of an abrupt stall development; to make this acceptable, one would possibly have had to introduce some variation in section shape across the span.

Turning now to slats B and C, neither of these proved to be an optimum configuration but nevertheless, the analysis of the results leads to some important general conclusions. The shape and position of the slat itself is the same in these two cases. It is merely the shape of the main wing upper surface near and downstream of the slot exit that is different (Fig.11). With slat B, there is a rapid change in slope near 0.12c and a forward facing step corresponding to the finite trailing edge thickness of the slat; with slat C, the change in slope is eased by a fairing undercutting the step. This change in geometry may appear to be small but the consequences are significant. Fig.13a shows that even at the moderate incidence condition of $\alpha = 8.7^{\circ}$, $C_L = 0.7$, i.e. more than 0.1 in C_L *below* the C_L for separation-onset for the clean wing, (Fig.12), a strong shock is already present on the main wing upper surface with both slats B and C but it has been weakened considerably by the change from B to C. With slat B, the suction reaches a maximum near the step and there is then some recompression ahead of the shock whereas with slat C, the fairing has eliminated the forward peak suction, and the local upstream Mach number (normal to the shock) ahead of the shock is about 1.26 as compared with 1.41 for slat B. Even with slat C however, a shock-induced separation is clearly imminent and so one must conclude that neither slat has been successful in postponing separation-onset relative to the clean wing. It is arguable that some improvement would

have been obtained if the fairing of slat C had been gentler and had extended over more of a chord. This has immediately highlighted two features of a good slat design for high Mach number: the change in direction imposed on the flow out of this slot exit and the curvature of the main wing surface downstream of this exit should both be kept as small as possible. This is equivalent to saying that the rear of the slat should be thin and that the slat trailing edge should be positioned as far aft as possible e.g. at about 0.18c rather than 0.12c. It is quite understandable that the optimum curvature of the surface between 0.2 and 0.3c should ideally be less than for a good clean wing design; in the latter case, when the flow is supercritical, the effect of the expansion waves from this part of the surface tends to be offset by the incoming compression waves reflected from the forward sonic line but at moderate incidences with the slat extended, the forward sonic point is further aft and these reflected compression waves will largely be absent.

It is clear therefore that it is difficult but not impossible to improve separation-onset at high subsonic speeds by means of a slat. Slats B and C do not achieve this but they are effective in controlling the subsequent development of the separation. As described in Section 2 above, with a clean wing with no leading-edge devices, when the incidence is increased beyond that for separation-onset, the shockwave moves forward towards the leading edge. Considering the wing as a whole, inboard of the separated area the shock front loses its sweepback, thus leading to an increase in shock strength and encouraging the separation to extend inboard. With a slat extended, however, as shown in Fig.13, the shock tends to remain in a position about 0.10 - 0.15c behind the slot exit. At higher Mach numbers, when the shock prior to separation is further aft, it moves forward under the influence of a separation to about this position but then again remains stationary for a sizable range of incidence. This is helpful in two senses: first, lift is maintained over the forward part of the main wing ahead of the shock and second, the shock retains its full sweepback. Also, as the incidence is increased, the lift on the slat itself continues to increase. A separate supersonic region forms and between $\alpha = 10.9^{\circ}$ and 13.1° this extends rearward towards the slat trailing edge. This rearward movement occurs first with slat C, i.e., it is influenced by the shape of the main wing leading edge. By $\alpha = 14.1^{\circ}$, Fig.13b, even with slat B the flow is supersonic back to the slat trailing edge but there is still a two-shock system with a pressure-rise ahead of the step on the main wing surface. With slat C on the other hand, the slat shock moves onto the main wing surface and coalesces

with the second shock. To judge from the C_L - α curves in Fig.12, this is a favourable development and so in these respects also, the shape of the main wing surface for slat C represents a distinct improvement over slat B. It should perhaps be mentioned however, that even here one has to compromise between requirements for different Mach numbers. At M = 0.65, slat C is to be preferred for the reasons stated; at lower Mach numbers, this applies to a greater extent because the peak suction near 0.12c for slat B is even greater and there is a premature separation due to the adverse pressure gradient behind this peak suction; at higher Mach numbers, on the other hand, the strongly triangular nature of the pressure distribution with slat C leads to worse drag characteristics, the drag-rise Mach number at moderate C_L being typically about 0.02 lower with slat C than with slat B.

This brief discussion of the results for slats B and C in Figs.12,13 suggests that in any assessment of the effectiveness of a slat at high Mach number, two incidences are of particular importance:

α_A : the incidence at which the shock-induced separation on the main wing extends to the trailing edge, and

α_B : the incidence at which the supersonic flow over the slat upper surface extends to the slat trailing edge.

For a good slat design, α_A should be as high as possible and α_B obviously should be nearly the same value. Slats B and C are poor in both respects. Even with slat C, $(\alpha_A - \alpha_B) = -3^\circ$ approximately and it is arguable that if supersonic flow at the slot exit has appeared by about α_A, much better control would have been exercised over the subsequent development of the stall. Further, if the supersonic flow over the slat can be achieved before α_A, the total lift carried at α_A would be greater. On these arguments, therefore, one suspects that the optimum value for $(\alpha_A - \alpha_B)$ should be slightly positive and this tentative conclusion has been borne out by an extensive, systematic research programme on different slat designs using the model illustrated in Fig.14. This is a half-model wing-fuselage configuration where for engineering convenience, the basic wing is untapered. The wing can be mounted at various angles of sweepback but is shown in Fig.14 set at 35° sweep fitted with the tip actually made for tests at 45° sweep. The slat supports are shown; through the use of different supports and wedge packing pieces, a wide range of slat deflections, extensions and gaps could be tested.

The results obtained at 25° sweep are summarised in Fig.15. The increments in maximum usable normal force ΔC_N (measured by the balance but assessed on the pressure plotting evidence) are plotted against the product $(x_{T.E.} g)$ and curves drawn through points for a given slat deflection δ. The symbols are defined in the sketch in the figure. At $M = 0.5$, a reasonable correlation is obtained showing that within the range tested, but not necessarily outside this range, increasing deflection, extension and gap tend to increase ΔC_N. At $M = 0.65$, however, it is a more complicated story. The best results, $\Delta C_N = 0.2$ are obtained as suggested above for configurations giving $(\alpha_A - \alpha_B)$ in the range 0° to 2°. Increasing the slat deflection and extension are only helpful while $(\alpha_A - \alpha_B)$ remains in this range; ultimately, $(\alpha_A - \alpha_B)$ becomes negative and the slat effectiveness then decreases. This is shown particularly by the sequence of results for $(x_{T.E.} g) = 16$ showing a reduction in ΔC_N as δ is increased from 5° to 15°, this increase in δ reducing the loading on the slat at a given incidence, thus increasing α_B and reducing $(\alpha_A - \alpha_B)$. The best slat designs give improvements of about $\Delta C_N = 0.2$, a notable achievement relative to the results for slats B and C discussed earlier since we are still considering the same Mach number (0.65), the same sweepback (25°) and a similar thickness/chord ratio. Another interesting point of detail about the results in Fig.15 is that the reduction of the slat gap has apparently produced an improvement. Analysis of the pressure plotting data showed that this was because the only significant change as the gap was reduced was in the pressures on the lower surface of the slat. These pressures increased thus giving more lift on the slat, but presumably, if the gap were decreased further, adverse effects would begin to appear. Thus once again, the lesson is that at the higher Mach numbers, the changes with any geometrical variable are no longer monotonic.

In the discussion in this section so far, the results have been analysed on a quasi-two-dimensional basis. With increasing Mach number and/or sweepback however, three-dimensional effects become important and this can be illustrated by presenting some results for the same model at 35° sweepback. Tests were made on the slat and droop (slat, slot closed) configurations shown in Fig.16. Results for the mid-semi-span pressure-plotting station A are presented for slat 1 in Fig.17 and in general terms although not in detail, this again illustrates the ability of the slat to control the development of the flow separation. A shock-induced separation bubble at the foot of the shock is first observed in condition 2; this extends back to the trailing edge by condition 3; the supersonic region on the slat extends back to the trailing edge of the slat

by condition 4; the coalescence of the two shocks occurs near condition 5 and some lift is maintained on the main wing ahead of the shock up to beyond condition 6. The shockwave is held behind the slot exit and thus retains a sweep near 35°; the shock-induced separation tends to roll up into a swept bubble or vortex-type flow and this leads to an improvement in the pressure recovery near $\alpha = 14^{\circ}$ between conditions 5 and 6 and thus to the increase in lift-curve slope in this range. The important extra feature in these results for 35° sweep however is the spanwise variation in slat effectiveness as shown in Fig.18. At the lower Mach numbers such as M = 0.5, it is not expected to find that the slat is successful in coping with the premature tip-stalling tendency of the clean wing but the more surprising results are those obtained at high Mach number where the slat is relatively ineffective near the tip but strongly effective near the root. Extending a slat can therefore be used to control not merely the forward but also the inward development of the area of flow separation.

The reasons for the variation in slat effectiveness across the span at high Mach number are not entirely clear but analysis of the pressure plotting results has shown that again, the trend can be interpreted in terms of the parameter $(\alpha_A - \alpha_B)$. As noted earlier, α_A depends primarily on the suctions generated in the supersonic region aft of the slot exit but typically, ahead of the wing maximum thickness. The suctions in this region are likely to be higher and as a consequence, α_A lower on the outer wing. Also, the results have shown that α_B is lower on the inner wing; the impression seems to be that on the outer wing, the rearward movement of the slat shock towards the trailing edge is delayed by a local flow separation over the rear of the slat. It follows that on both counts, $(\alpha_A - \alpha_B)$ tends to be positive on the inner wing and negative on the outer wing. Clearly, one would welcome a better result on the outer wing than that obtained with slat 1 because separation-onset for the wing as a whole will be at a lower C_L at high Mach number than for the clean wing, but on the other hand, even when this happens, the slat still retains its ability to control the development of the separation as shown graphically by the shape of the $C_L - \alpha$ curves for M = 0.80 in Fig.18.

The overall results for all the configurations at 35° sweep are presented in Fig.19. It will be seen that substantial improvements are achieved at M = 0.50 and even more so, in the case of slat 1, at M = 0.65 but there is then a deterioration at the higher Mach numbers. This figure has however been included

not so much to show the actual increments in useable lift due to each configuration but illustrate that with the slats particularly, because of the gradual development of the flow separations, it may be impossible to quantify these increments merely on the basis of the breaks in the overall C_L (or C_N) curves. To take for example the results for slat 1 at M = 0.75, one would certainly not expect the maximum usable C_N to be better than about C_N = 1.18 just past the major break in the $C_N - \alpha$ curve but an analysis of the pressure plotting data and the unsteady output from wing root bending moment gauges suggests that moderate buffet, and hence possibly an operational limit, may be as low as C_N = 0.97 or only 0.10 above the assessed value for the clean wing. Setting the limit at this point would imply reverting to condition 3 on Fig.17. This may appear contradictory in that one is not taking advantage of the ability of the slat to maintain lift over the forward part of the wing up to condition 6 but this is not so because the performance of the wing as a whole is being degraded by what is happening outboard of station B. It is worth pointing out that the adverse effects on the outer wing may be particularly pronounced in this example because the results have been obtained for an untapered wing with a far from ideal tip shape. In practice, with a real aircraft having a tapered wing, some twist and a properly designed planform and section shape near the tip, the adverse effects could be much less pronounced and then one would be able to capitalise on the separation control evident at station B.

To summarise, a slat designed with careful attention to the shape of the main wing surface near and downstream of the slot exit can improve separation-onset except possibly near the tip up to quite high Mach numbers but the main virtue of a slat at high Mach number is in controlling the forward and inward spread of the flow separation and thus, improving the buffet penetration qualities. The more it is successful in this aim, the more uncertain becomes the assessment of the true maximum usable lift. More research is needed on this point.

4 THE USE OF VARIABLE GEOMETRY WING PROFILES

After all that has been said in the preceding sections the advantages of being able to change the actual profile shape at will to suit the various aerodynamic conditions as they arise at different points in the flight envelope are fairly obvious. We are a very long way off from this ideal situation, of course, but a small advance has been made by the recent development within

the UK of a linkage system able to control surface shape locally from within the wing. This device has been called the 'Royal Aircraft Establishment Variable Aerofoil Mechanism' or 'RAEVAM' for short.*

4.1 The RAEVAM device

The starting point for this idea was the development of a new type of variable liner for the working section of a supersonic tunnel at RAE[4] to meet a requirement for a fast and accurate system to use in conjunction with a 'dynamic simulator'[5]. Fig.20 shows the finished system now in operation. The flexible walls of the working section are positioned by a large number of stiff links pivoted at one end at points along the walls and at the other on rigid earth-frames. The forward and rear ends of each flexible wall are free to slide fore and aft at the points where they blend with the fixed walls of the nozzle, and suitable sliding joints have been designed to avoid any disturbances locally. The lengths of the links and the position of the pivots on the earth frame were chosen so that as the flexible walls are moved fore and aft by means of a hydraulic jack, the required range of liner shapes is formed. The geometry of the linkage system is in fact completely determined by specifying the exact shape of the walls required at *three* specific points in the range, but choosing these points with care it was found in practice that the liner shape between these design points gave as good quality tunnel flow at intermediate Mach numbers as achieved normally with fixed liner blocks.

This principle has now been applied to the surface profiles of wings. In this paper we are concerned with changes of profile at the leading edge, and in particular with the need to vary the shape in this region through the high subsonic speed range to improve lift performance at the stall. A typical installation is shown in Fig.21. The leading edge is conveniently left solid and is constrained by the arm 'A' to rotate about some point P. The rest of the skin is made flexible and is constrained in shape by means of a series of links pivoted at the underside of the skin at one end and at various points on an extension to the main spar at the other. The ends of the flexible skin slide in sealed joints where they blend with the main fixed parts of the wing profile. Variation of the profile shape is achieved by means of a single jack, 'J', rotating the leading edge frame, pivoted at P. As with the wind-tunnel liner, the lengths and pivot positions of the links are determined by

*Patent rights have been filed under Patent Application No. 27787/69

specifying three precise nose shapes required. In the studies we have made so far, we have generally taken one of these shapes as that extreme droop position needed for low-speed C_{Lmax} and the other two as those needed to meet two particular requirements of high-lift performance at high speeds. The variation of profile shape between these design points is, of course, always smooth and progressive and appears to raise no problems in practice. There are, however, some practical constraints to consider. For instance, the position of the pivots at the fixed ends of the links must lie within the profile, but the links can be allowed to cross each other so there is a surprising amount of design freedom to accommodate the types of profile change typically required.

Several variations to this first simple mechanism described above are possible, but need no more than a mention here. It is perhaps worth noting that the system shown in Fig.21 always implies a shortening of the chord as profile nose-down camber is increased. The installation shown in Fig.22 however, shows how with the small extra complication of an extra motion controlled by a second jack, some forward extension of the leading-edge can be included in the variable geometry. Other subsidiary motions can include rotation of the whole leading edge about a second pivot as shown in Fig.23. In this case only one sliding joint is needed at the blend point between the flexible and fixed areas of the skin.

4.2 Aerodynamic considerations

If we refer back for a moment to Fig.1 in this paper it is interesting to speculate on what a variable-geometry device such as RAEVAM can do to improve performance at the stall over the high-subsonic speed range. The three typical pressure distributions quoted before are given again in Fig.24 and the diagramatic effects of nose droop are sketched in with dotted lines. At the low end of the speed range, the height of the leading-edge suction peak and the strength of the associated shock wave can be effectively reduced by nose-down changes to the leading-edge profile. This, as we have seen previously is beneficial since the incidence for the stall is increased and hence the value of C_{Lmax} achieved. At the high end of this speed range the application of small nose-up changes in profile can counteract the basic tendency for triangular types of supercritical pressure distribution to arise. Not only can prescribed peaks at the start of the supercritical region be induced to appear to improve the local lift directly, but the whole of the development of the supercritical flow up to the shock can be manipulated by this means. For the

same shock strength considerably more lift can thus be carried by the proper use of such profile modifications. At intermediate Mach numbers, however, provided the original profile design was a reasonably good one, there is probably little that can be done directly by the use of shapes generated by the RAEVAM device. Down-droop of the leading edge will basically tend to strengthen the shock (at fixed incidence); the opposite will tend to make the supercritical pressure distribution too 'peaky', the latter resulting perhaps in multishock systems and (at best) worse boundary-layer conditions at the main shock and further aft along the wing chord. In practice it has been found that the benefits of nose-down droop at the lower Mach numbers and of nose-up changes at the higher Mach numbers can overlap in the speed range, thus avoiding these difficulties at intermediate conditions.

On the complete wing, as we have seen in earlier parts of this paper, there is not only a need for a variation of leading-edge profile with Mach number, but variation is also desirable across the wing span to cope with the strong three-dimensional effects which can arise at near-stalling conditions. This raises engineering complications in the use of any moving leading-edge device, but it is comforting to note from the preceding discussion on the use of slats that leading-edge devices can change, and thus be used to control, the spanwise development of flow separation even when no spanwise grading of the geometry is employed. Perhaps the best approach to the problems of spanwise variation in stalling behaviour at high speeds lies initially in the spanwise variation of the shape and thickness of the basic profiles used in the wing design coupled with some incorporation of wing twist and a proper use of the inevitable effects of aeroelastic distortion. However a limited degree of spanwise variation in the settings of variable-geometry devices may be desirable in addition to this. Continuous variation of such settings across the span should not be ruled out in the future as we become more and more able to cope with the engineering complications involved, but for the present we probably have to content ourselves with discontinuities across the span which bring with them their own problems.

4.3 Recent test results at high speeds

The data shown in Figs.25, 26 and 27 have been included to demonstrate the use of the RAEVAM device at high speeds to improve the stall boundary of a wing profile. The section used with the leading-edge modifications tried is shown at the bottom of Fig.25. The solid leading-edge piece was restricted to 2% chord in this case and a blend-point with the main profile shape was selected at 18% chord. The shapes, which were tested in the 2ft x 1½ft tunnel of RAE,

were compatible for the pivot position shown with a practical linkage system of the type shown in Fig.21. The results of the 5^{o}-down and $1\frac{1}{2}^{o}$-up modifications to the section are given in the top figure and show how the benefits achieved at low speed and high speed overlap in the speed range near M = 0.65. The inference from this figure is quite clear: the whole boundary has been improved over all the range of high subsonic Mach number from M = 0.5 to M = 0.75.

Figs.26 and 27 show some samples of the pressure distributions measured during these tests. In Fig.26, the small $1\frac{1}{2}^{o}$ nose-up variation was adverse at M = 0.6 as expected, the shock being strengthened and moved forward on the chord (note also the deterioration of the trailing-edge pressure). At M = 0.75 this change in the profile geometry was beneficial, extra suctions being developed before the shock which itself was virtually unaffected in strength. In Fig.27, the 5^{o} down-droop variation in geometry both lowers and spreads the suction peak as expected at M = 0.5 resulting in an increase in stalling incidence and C_{Lmax}. At M = 0.7, however, the effects are adverse since the main shock is considerably strengthened at constant incidence resulting in earlier flow separations as incidence is increased.

From this initial pilot set of measured data, it can be said that the use of this variable-geometry device shows great promise in the context of the aerodynamic problems discussed in this paper. Studies in connection with the use of the device to improve C_{Lmax} at low speeds are proceeding in parallel with further work at high speeds, and a review is being made of the structural problems likely to arise in the incorporation of the device on an actual aircraft wing.

5 CONCLUSIONS

This paper has emphasized by means of some recent examples of research work the critical importance of the geometry of the leading edge as regards the stalling characteristics of wings at high subsonic speeds. To match performance over a range of these speeds some use of variable geometry is needed and the use of devices such as leading-edge slats raise their own problems of making compromises across the speed range. More work is wanted to enlarge our understanding of the particular supercritical aerodynamic flows associated with the use of such devices in both two-dimensional and three-dimensional situations.

In parallel with this is the need to develop better devices fundamentally more suited to the basic design processes of wings and more able to cope with the complexities of the flows which develop near leading-edges at high incidence at these high speeds.

NOTATION

Λ	sweepback angle of wing
c	chord of wing section
$\bar{c}$	mean chord of wing
C_N	normal-force coefficient
C_L	lift coefficient
C_p	surface pressure coefficient
p	static pressure
H_0	total pressure, free stream
M	Mach number
α	angle of incidence
x	distance along wing chord
η	proportion of wing semi-span
δ	angular rotation of slat, deg
g	slat gap, at slat trailing-edge, % chord
$X_{T.E.}$	forward extension of slat trailing-edge, % chord

REFERENCES

No.	Author	Title, etc.
1	H.H. Pearcey J. Osborne A.B. Haines	The inter-action between local effects at the shock and rear separation - a source of significant scale effects in wind-tunnel tests on aerofoils and wings. AGARG CP 35, Paper 11 (1968)
2	E.W.E. Rogers	An introduction to the flow about plane swept-back wings at transonic speeds. J. Roy Aero Soc 64, 449-464 (1960)
3	I.M. Hall E.W.E. Rogers	Part I: The flow pattern on a tapered sweptback wing at Mach numbers between 0.6 and 1.6. Part 2: Experiments with a tapered sweptback wing of Warren 12 planform at Mach numbers between 0.6 and 1.6. ARC R & M 3271 (1960)
4	D. Pierce	A simple flexible supersonic wind tunnel nozzle for the rapid and accurate variation of flow Mach number. ARC CP No.865 (1965)
5	L.J. Beecham W.L. Walters D.W. Partridge	Proposals for an integrated wind tunnel - flight dynamics simulator system. ARC CP No.789 (1962)

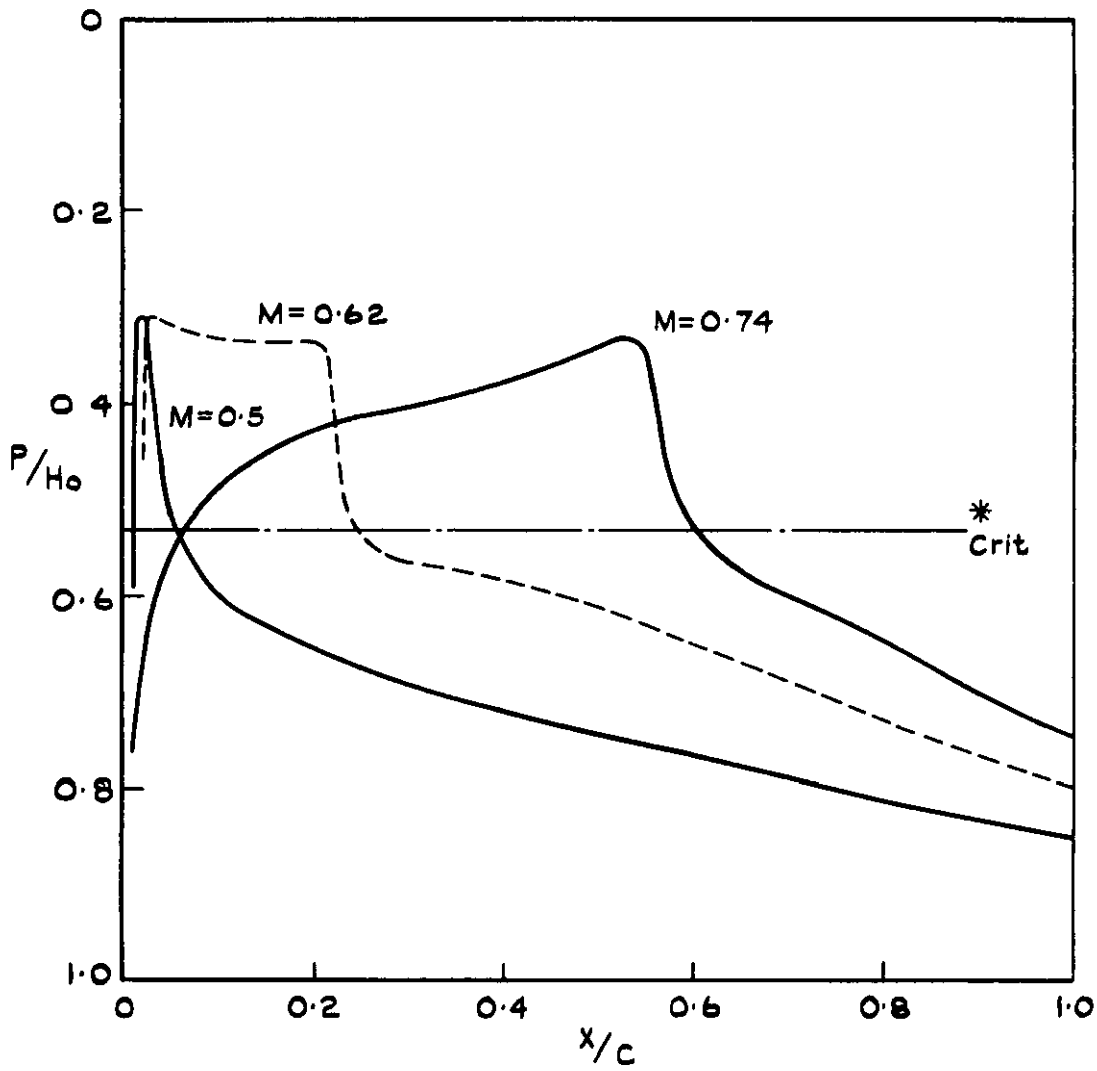

Wing section 'A'

M = 0·50	α = 8°	C_L = 1·06
0·62	6°	1·02
0·74	2°	0·54

Fig. 1 Basic types of upper-surface pressure distributions at super-critical conditions before flow breakdown

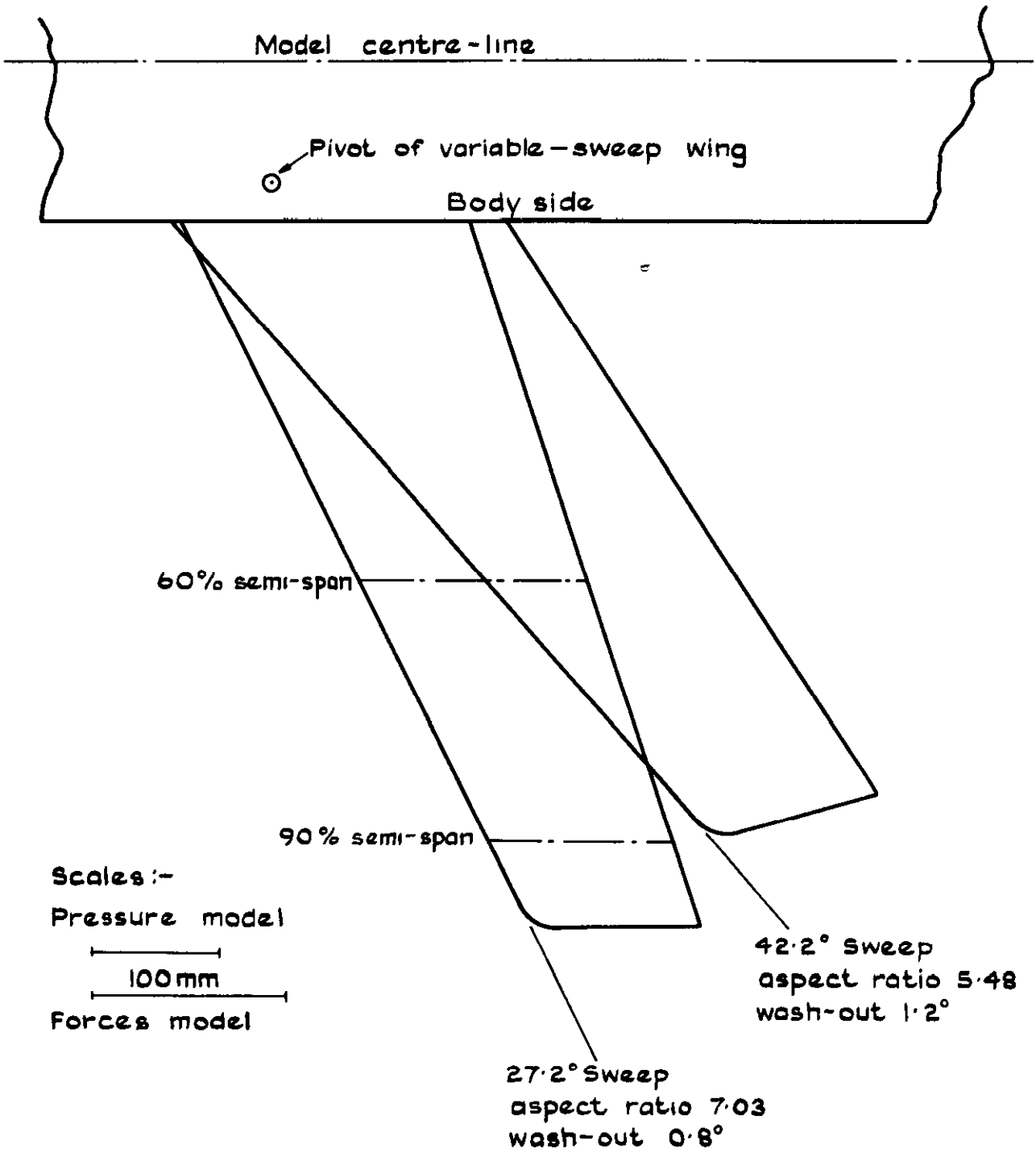

Basic wing section 'A' (perpendicular to quarter-chord line)

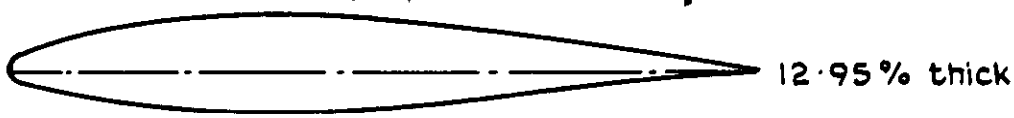

Test Reynolds numbers, based on mean chord, 27·2° sweep:-
pressures, $2{\cdot}4 \times 10^6$: forces, $1{\cdot}4 \times 10^6$: 2 dim tests, $6{\cdot}5 \times 10^6$

Fig. 2 Details of the geometry of the variable-sweep wing used to obtain the data of figs 7 and 8

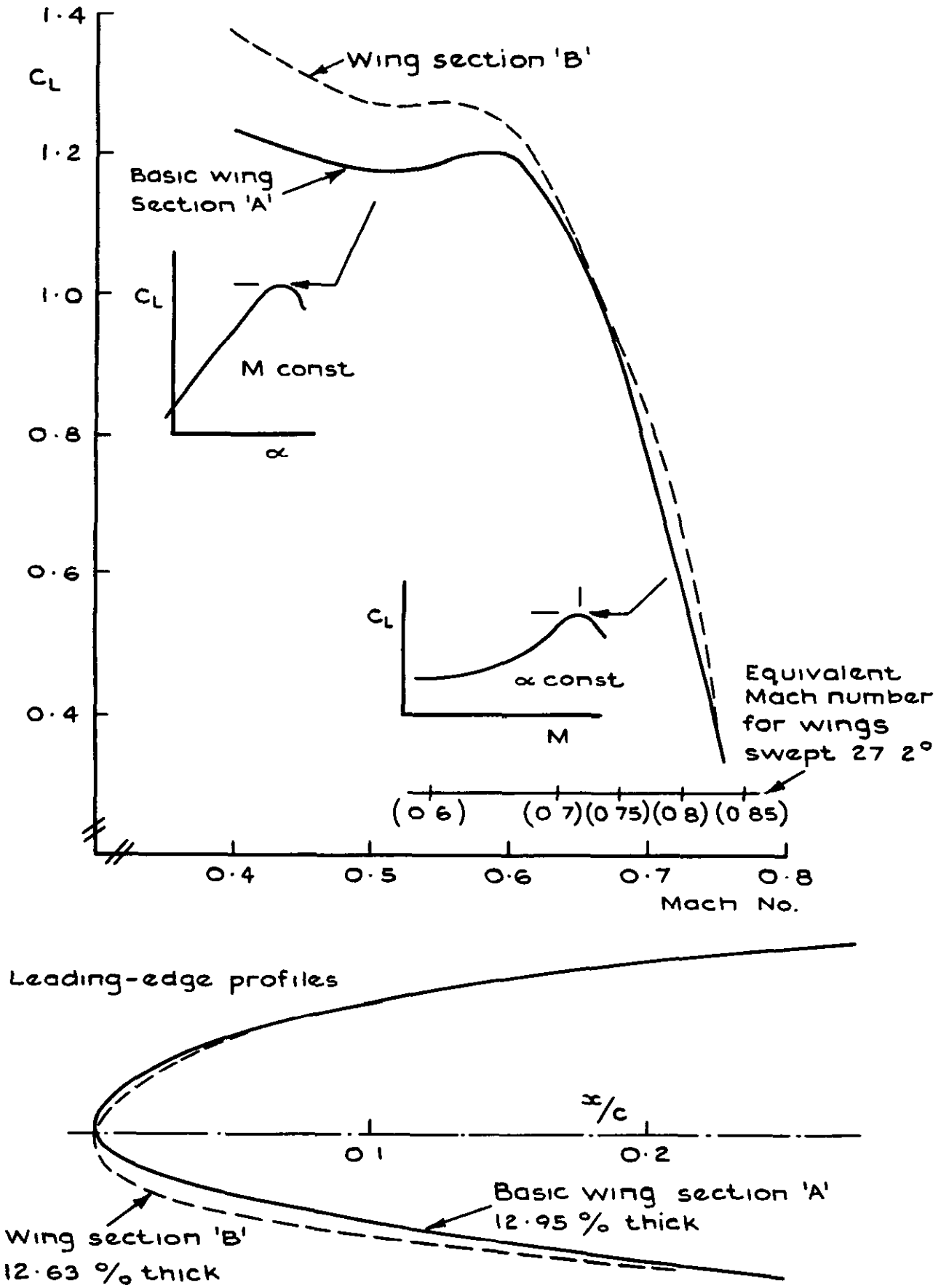

Fig.3 Stall boundaries from two-dimensional tunnel tests on wing section 'A' and on the modified section 'B'

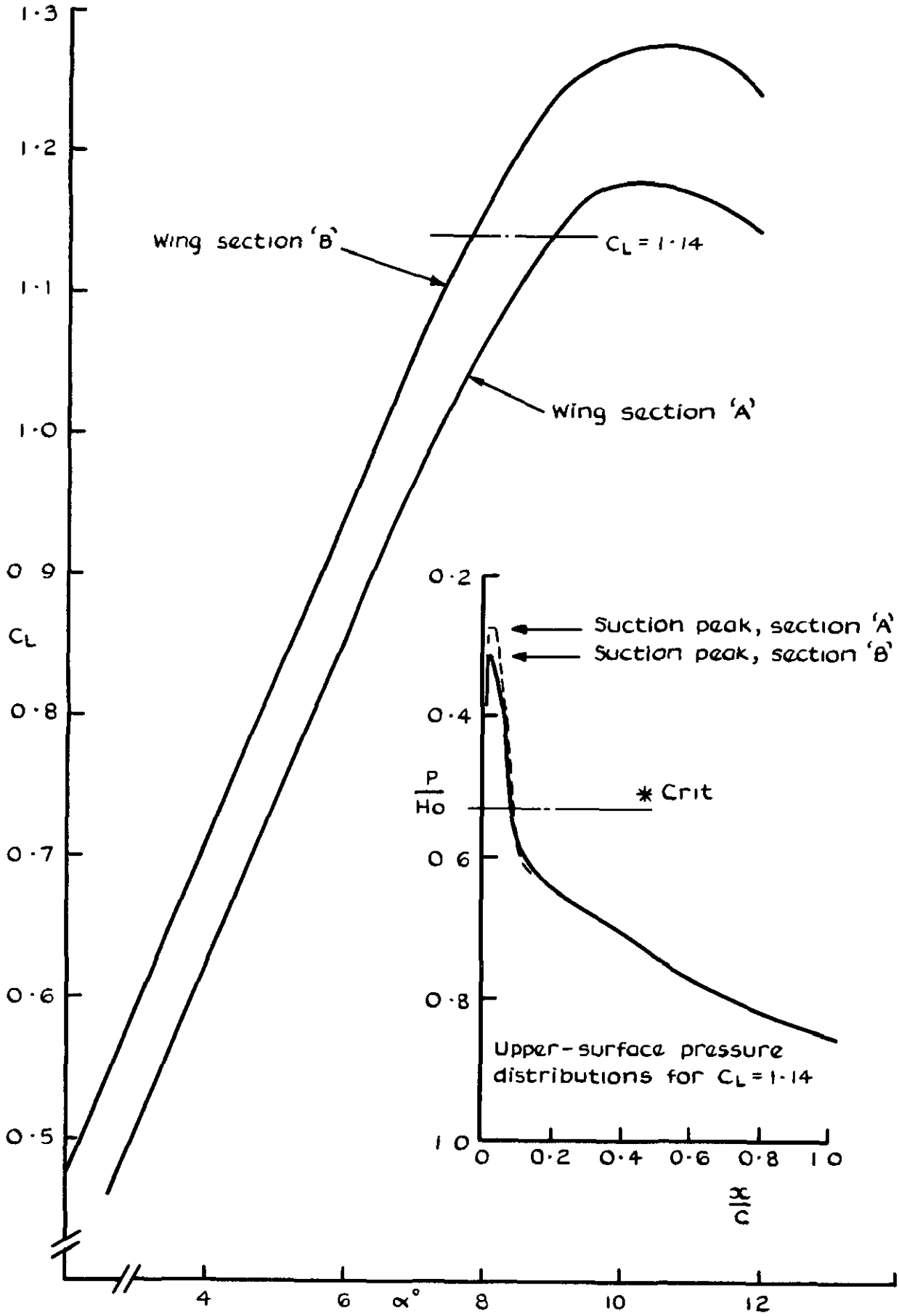

Fig.4 Characteristics of wing sections 'A' and 'B' at M=0·50

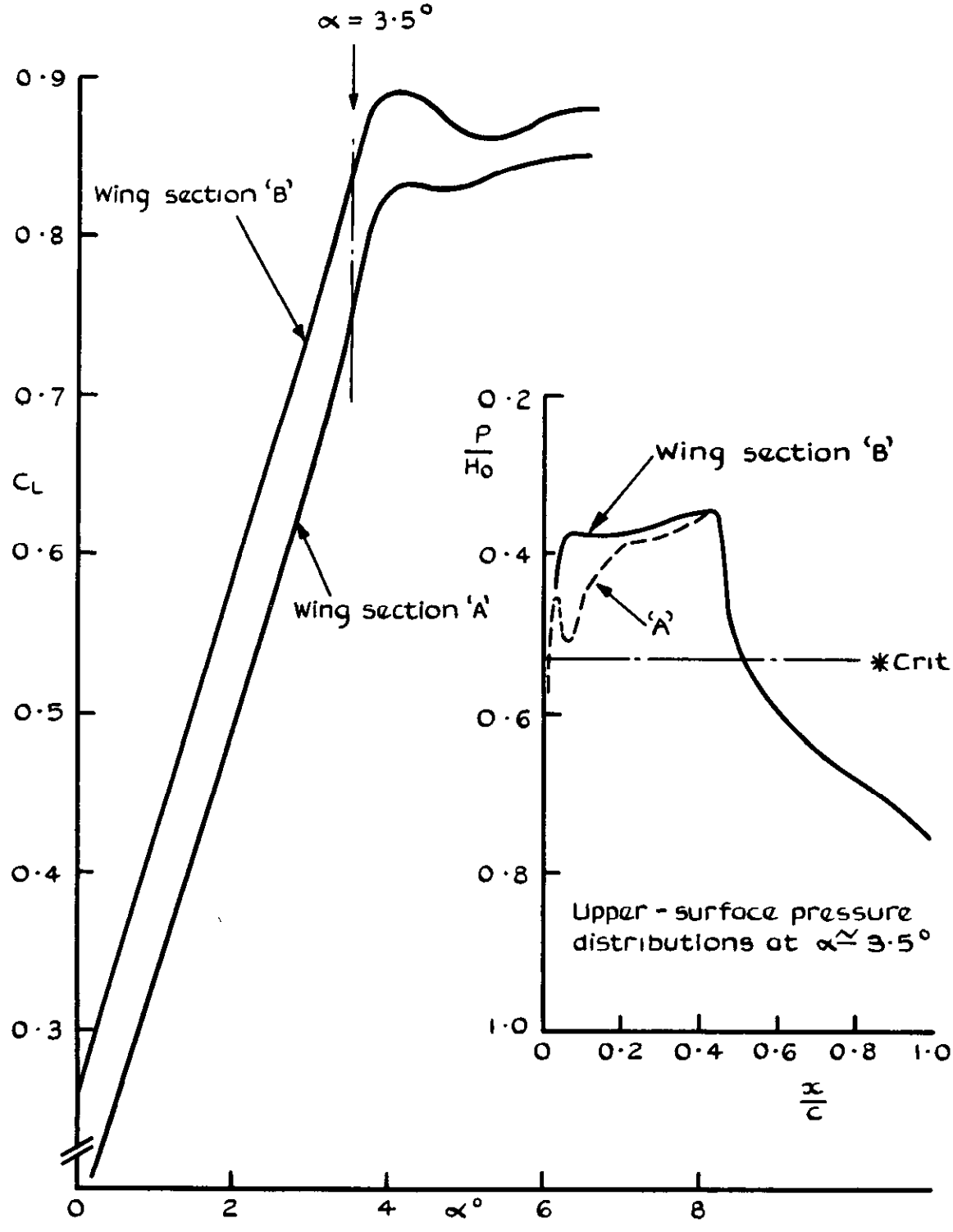

Fig. 5 Characteristics of wing sections 'A' and 'B' at M=0·70

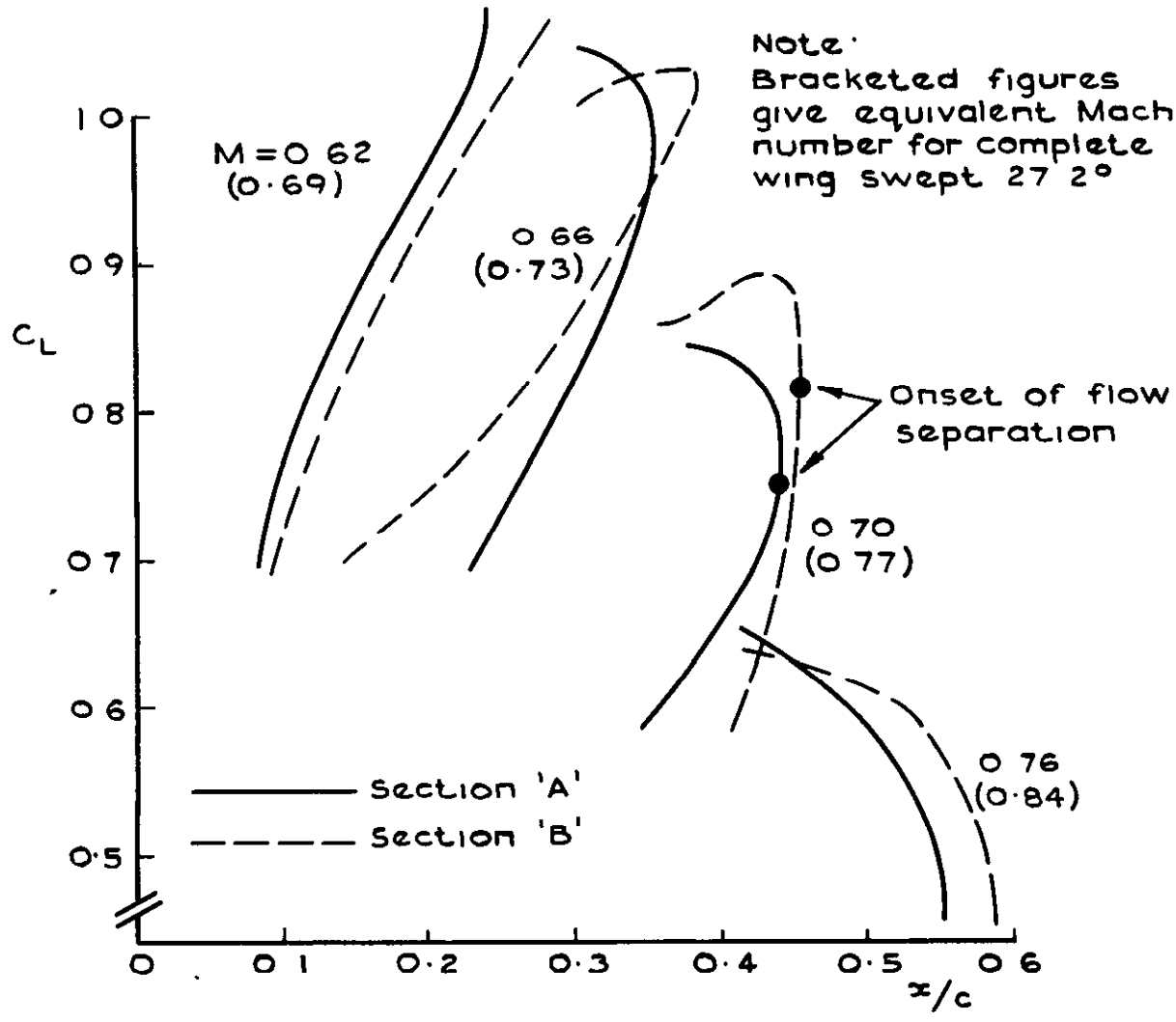

a Upper-surface shock position

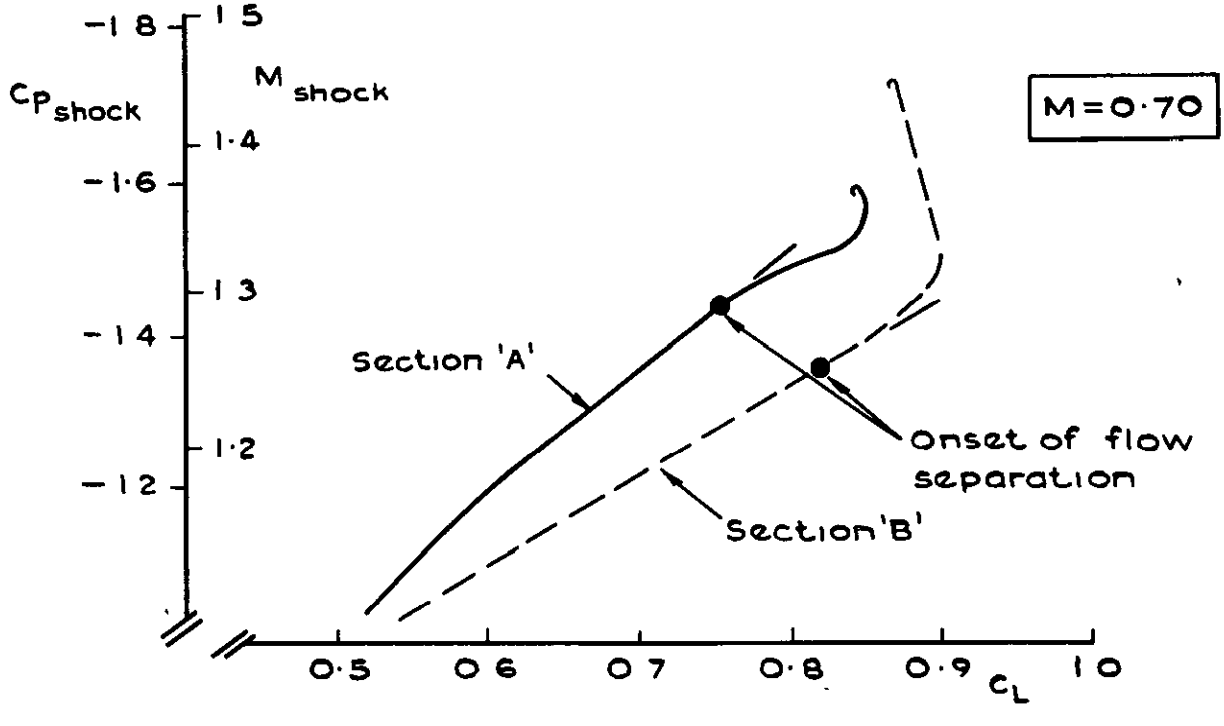

b Upper-surface shock strength

Fig.6 a&b Upper-surface shock position and strength from two-dimensional tests on wing sections A and B

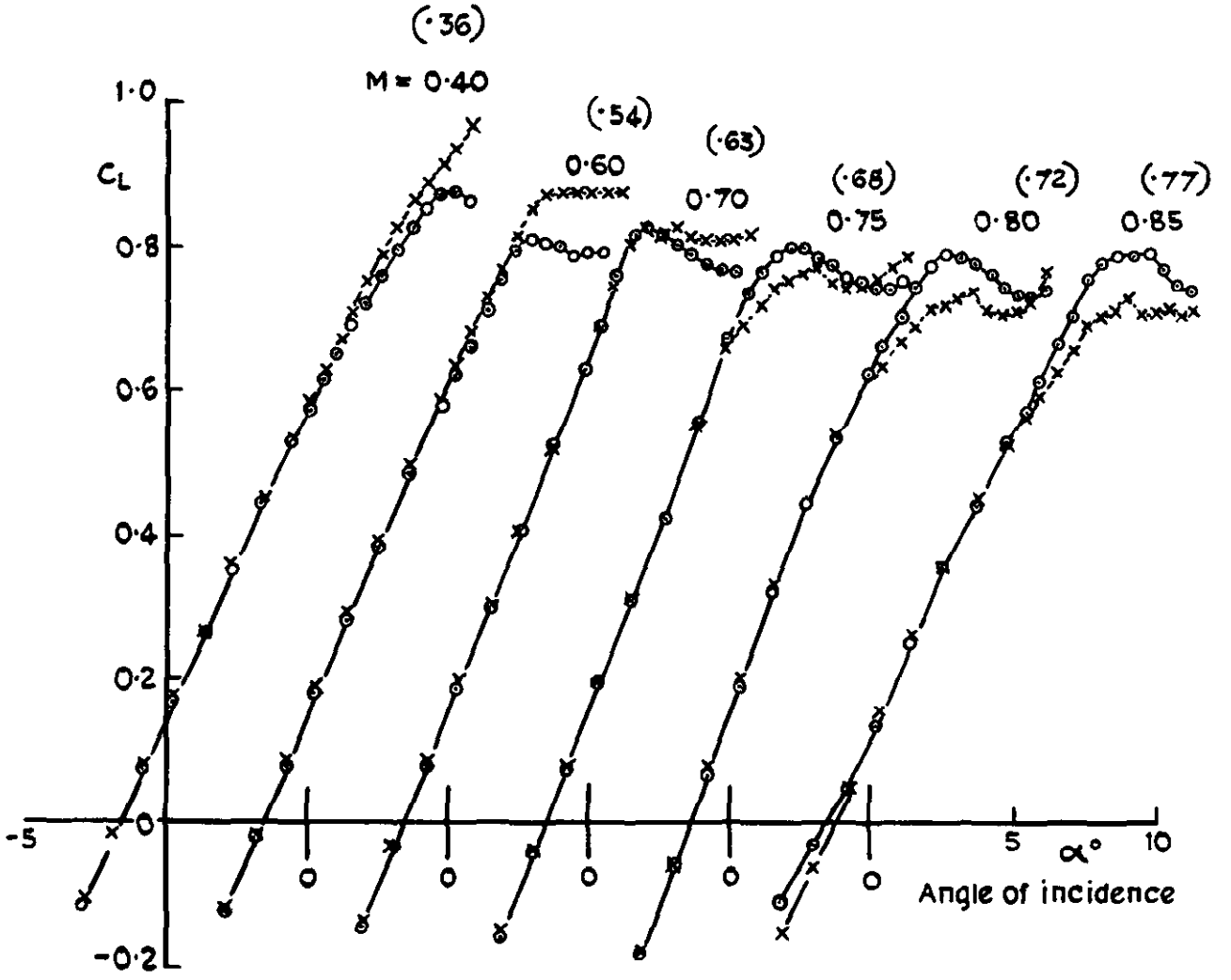

Approximate equivalent 2-dimensional Mach number given in brackets

—⊙— : Wing section 'A' —×— : Wing section 'B'

Fig.7a Lift-curves for complete model with wings swept 27·2°

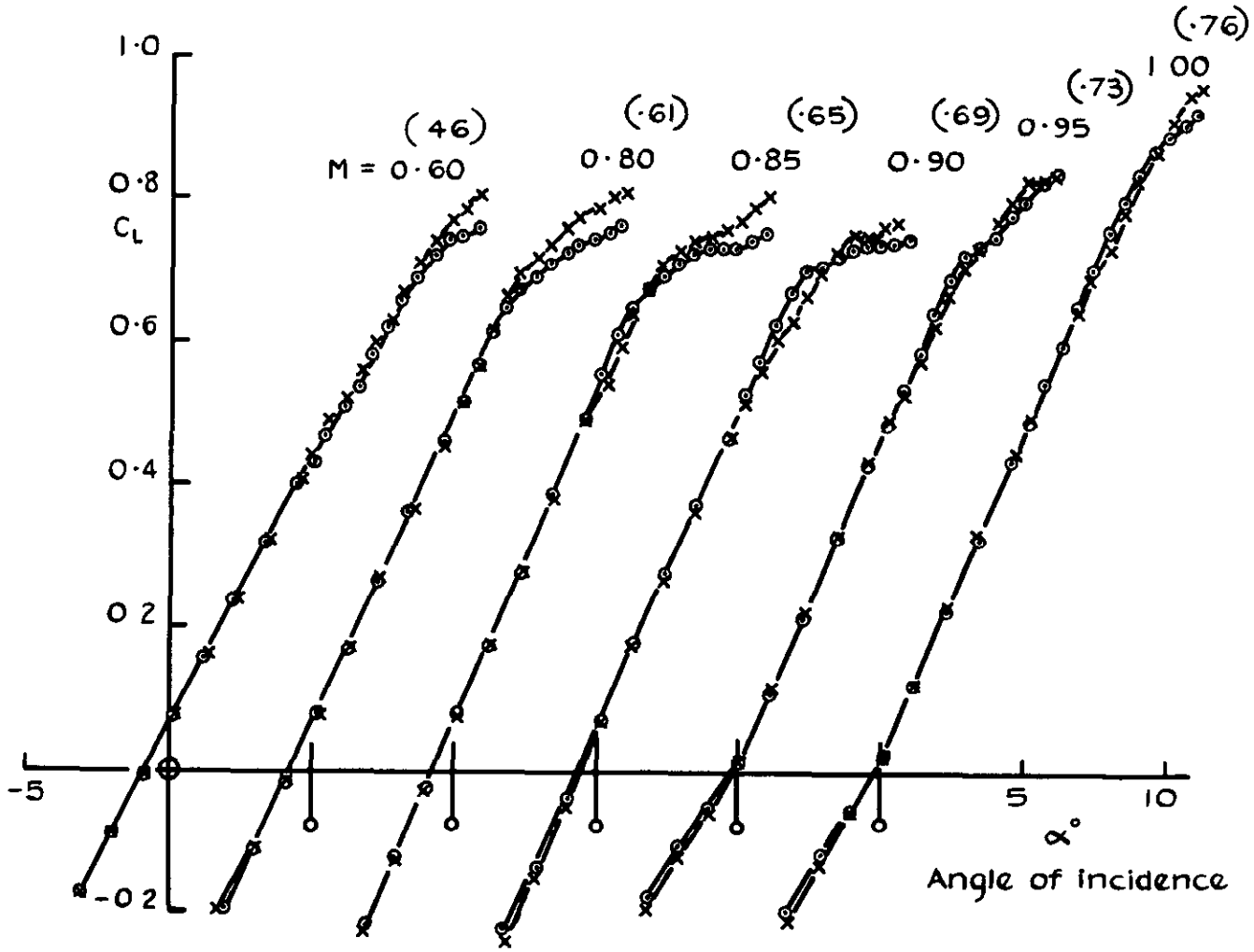

Approximate equivalent 2-dimensional Mach number given in brackets
—o— Wing section 'A', —x— Wing section 'B'

Fig.7b Lift-curves for complete model with wings swept 42·2°

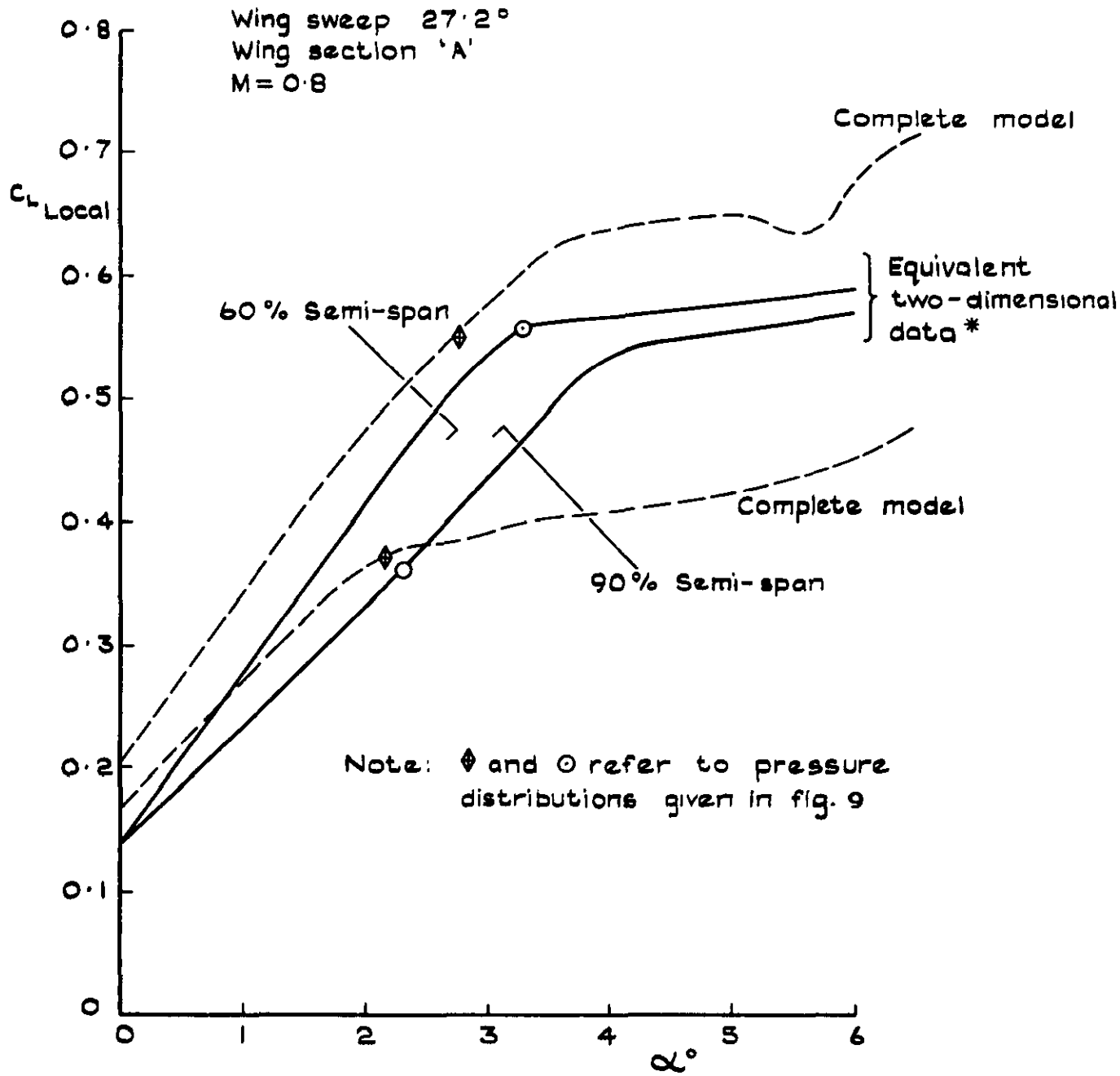

Complete model with wings swept 27·2°, M = 0·8
Two-dimensional data at M = 0·72 shown for comparison

*Note: The two-dimensional data includes allowances for body-upwash and induced incidence

Fig. 8 Comparison between local-lift curves at M = 0·80 for the complete model configuration and for the equivalent two-dimensional data at two spanwise positions

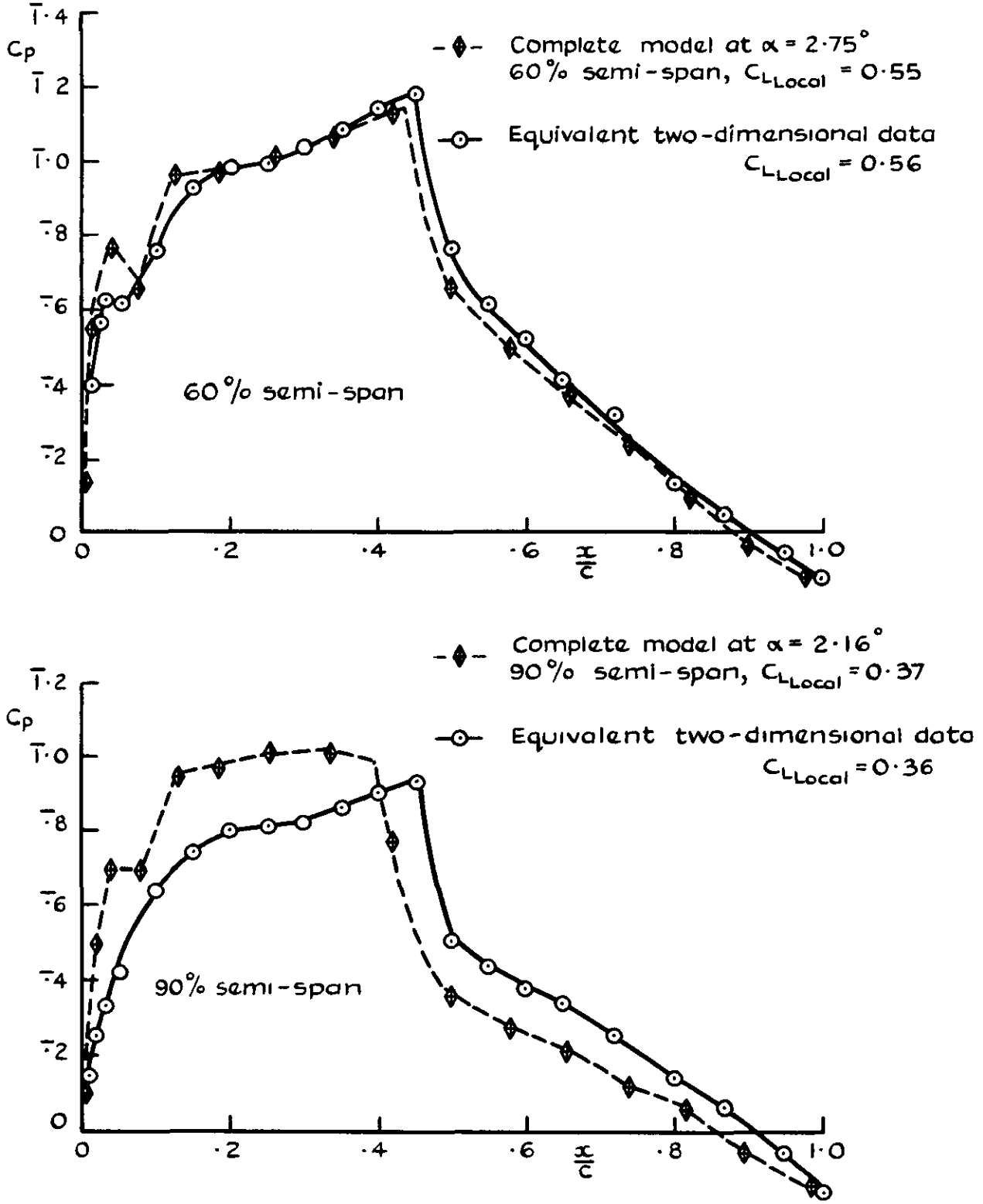

Fig. 9 Comparison between chordwise pressure distribution at M=0·80 for the complete model configuration and the equivalent two-dimensional distribution at the same local lift-coefficient

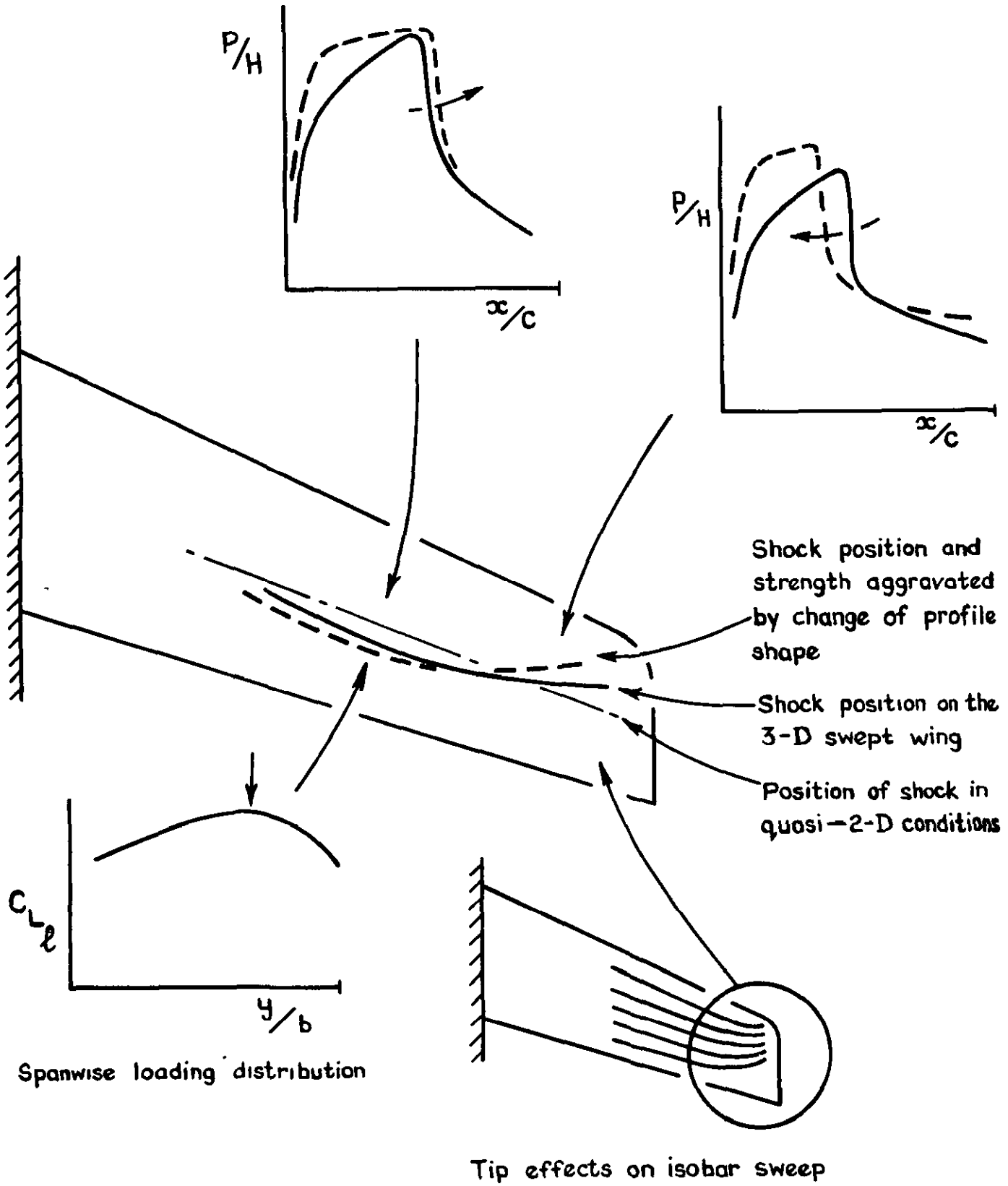

Fig.10 Effect of the profile modification on upper surface shock position (Diagrammatic only)

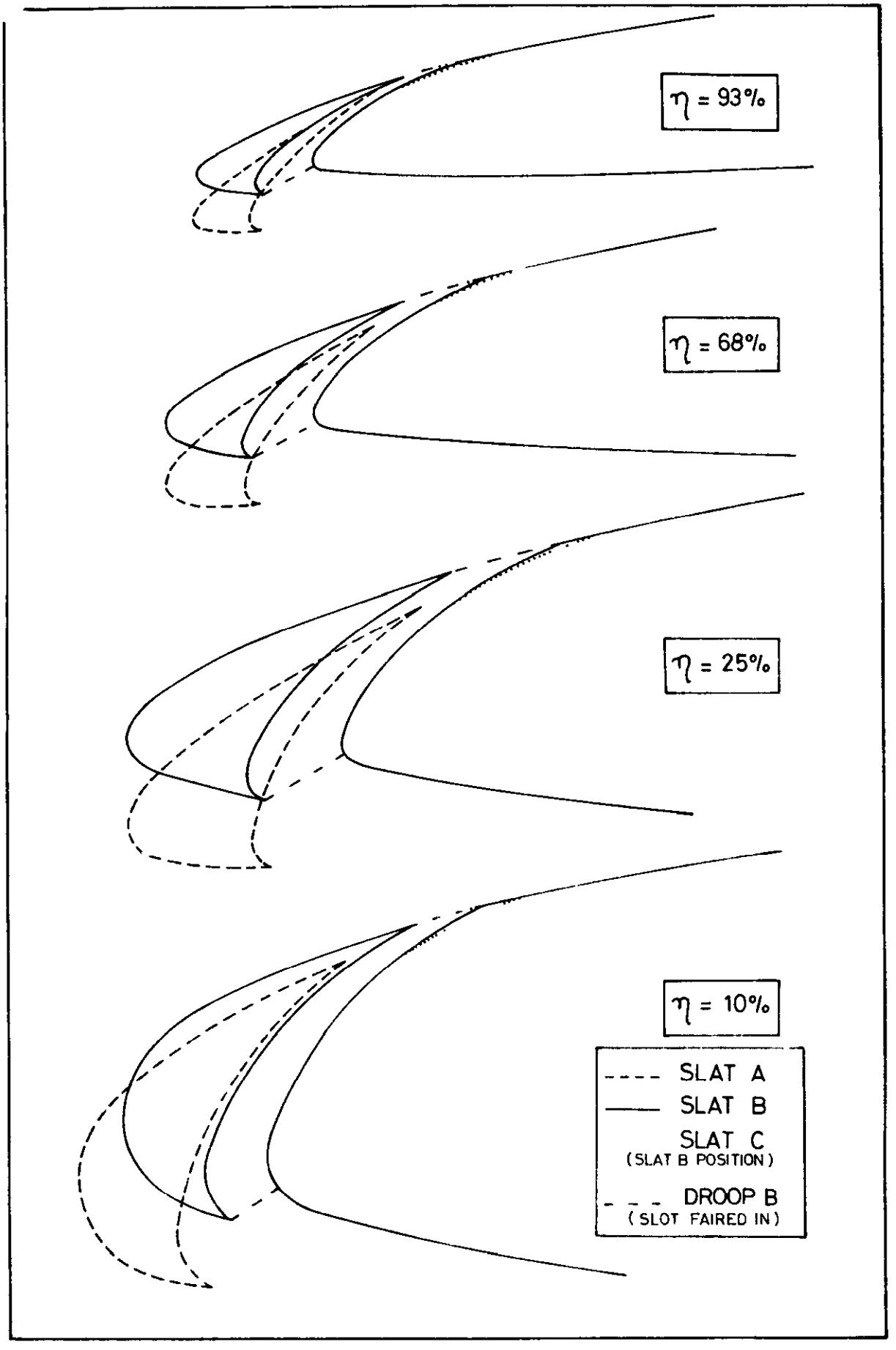

FIG. 11 SLAT DESIGNS · DIFFERENT STATIONS ACROSS SPAN OF 3D SWEPT WING

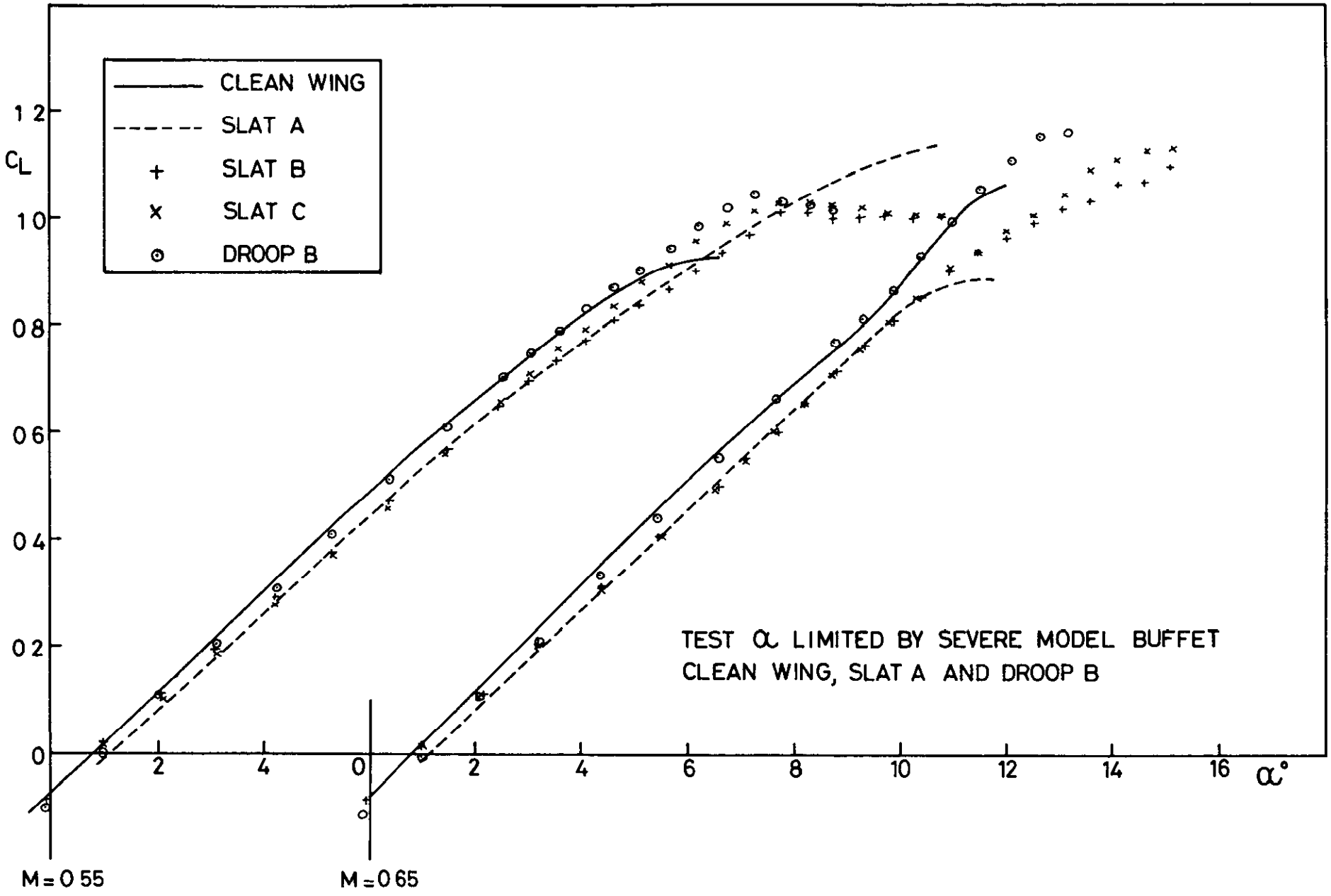

FIG. 12 EFFECT OF SLATS AND DROOPED NOSE ON OVERALL LIFT OF 3D WING

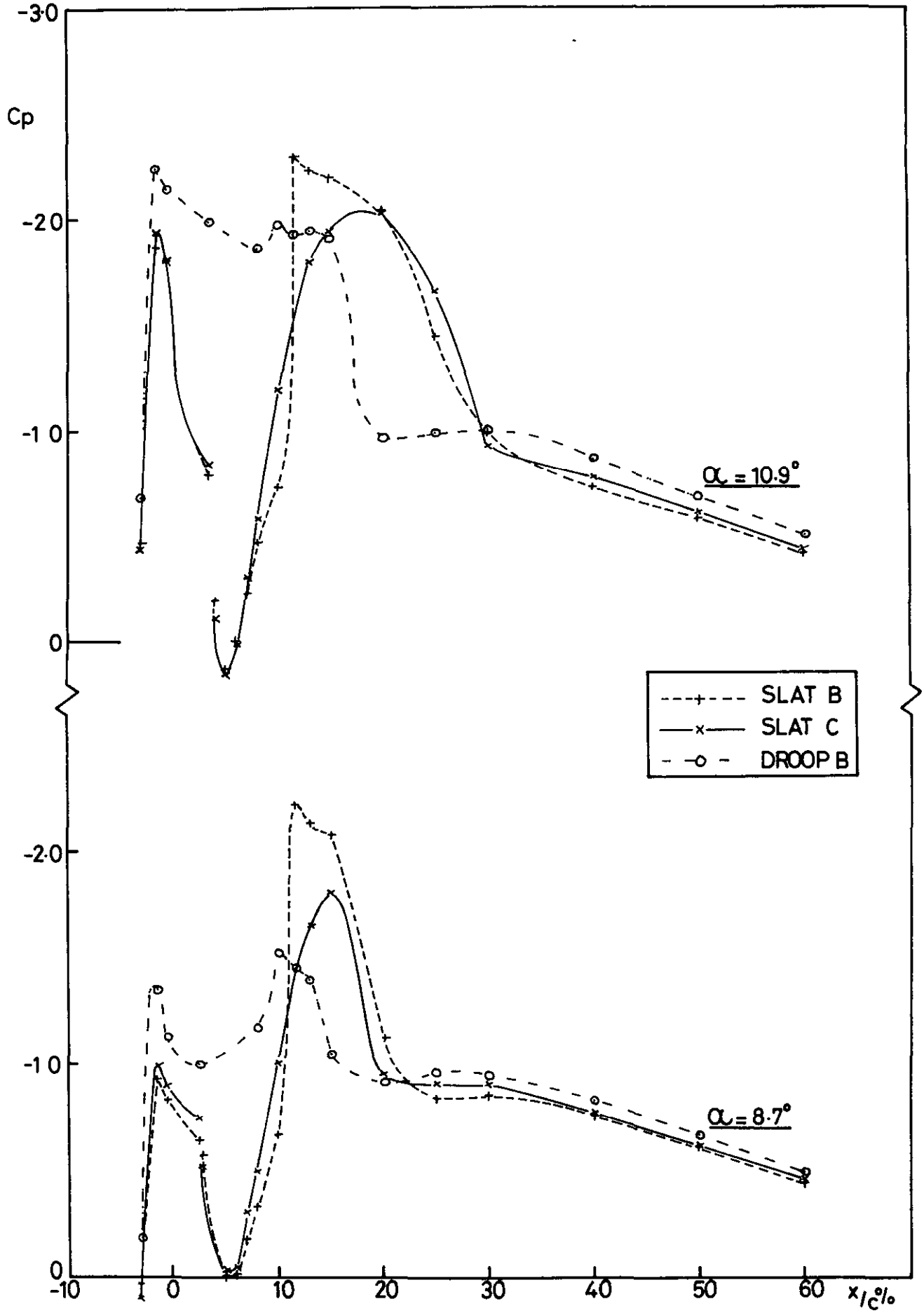

FIG. 13a FORWARD PRESSURE DISTRIBUTIONS:
M = 0·65, 0·5 x SEMISPAN

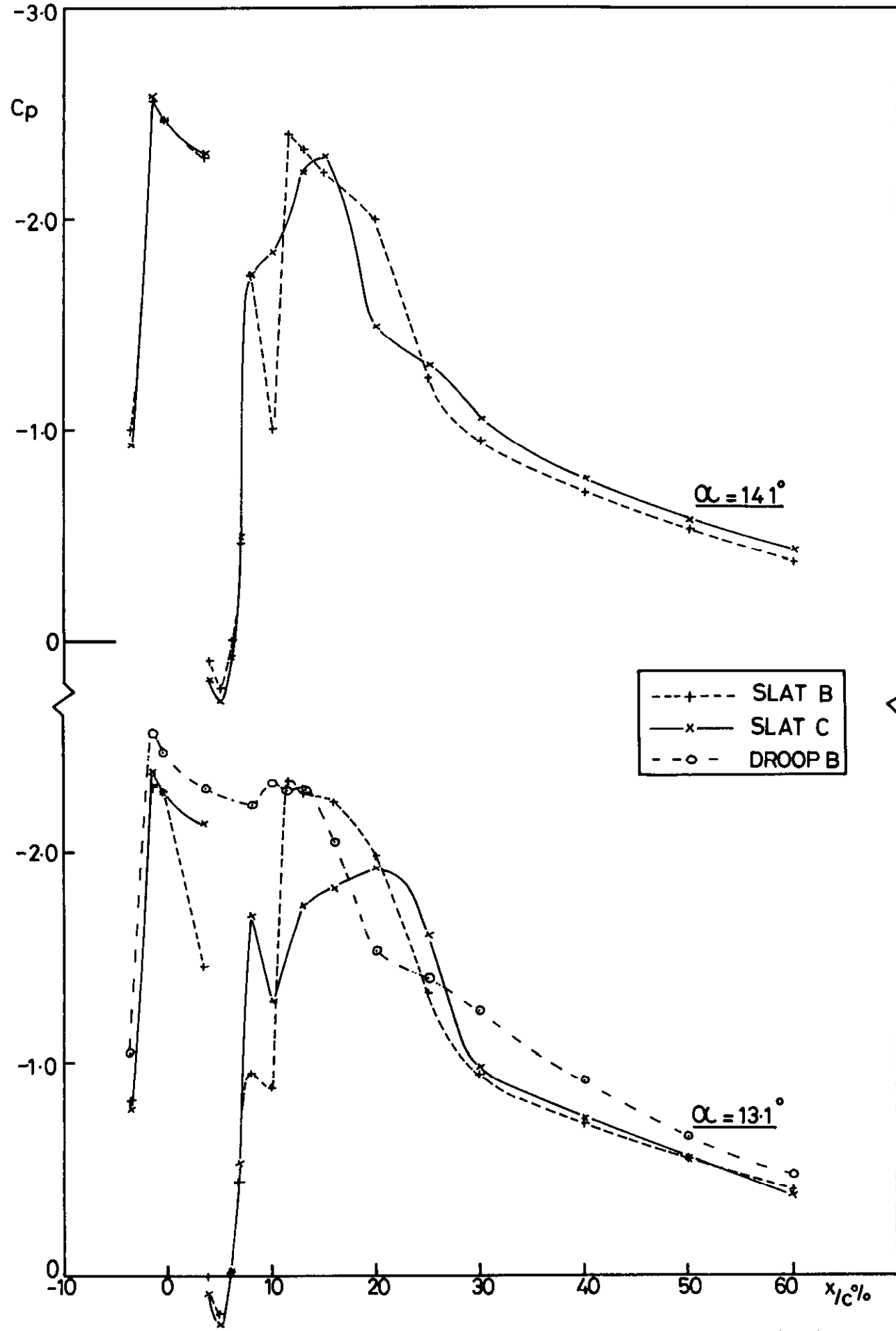

FIG. 13b FORWARD PRESSURE DISTRIBUTIONS: M = 0·65, 0·5 x SEMISPAN

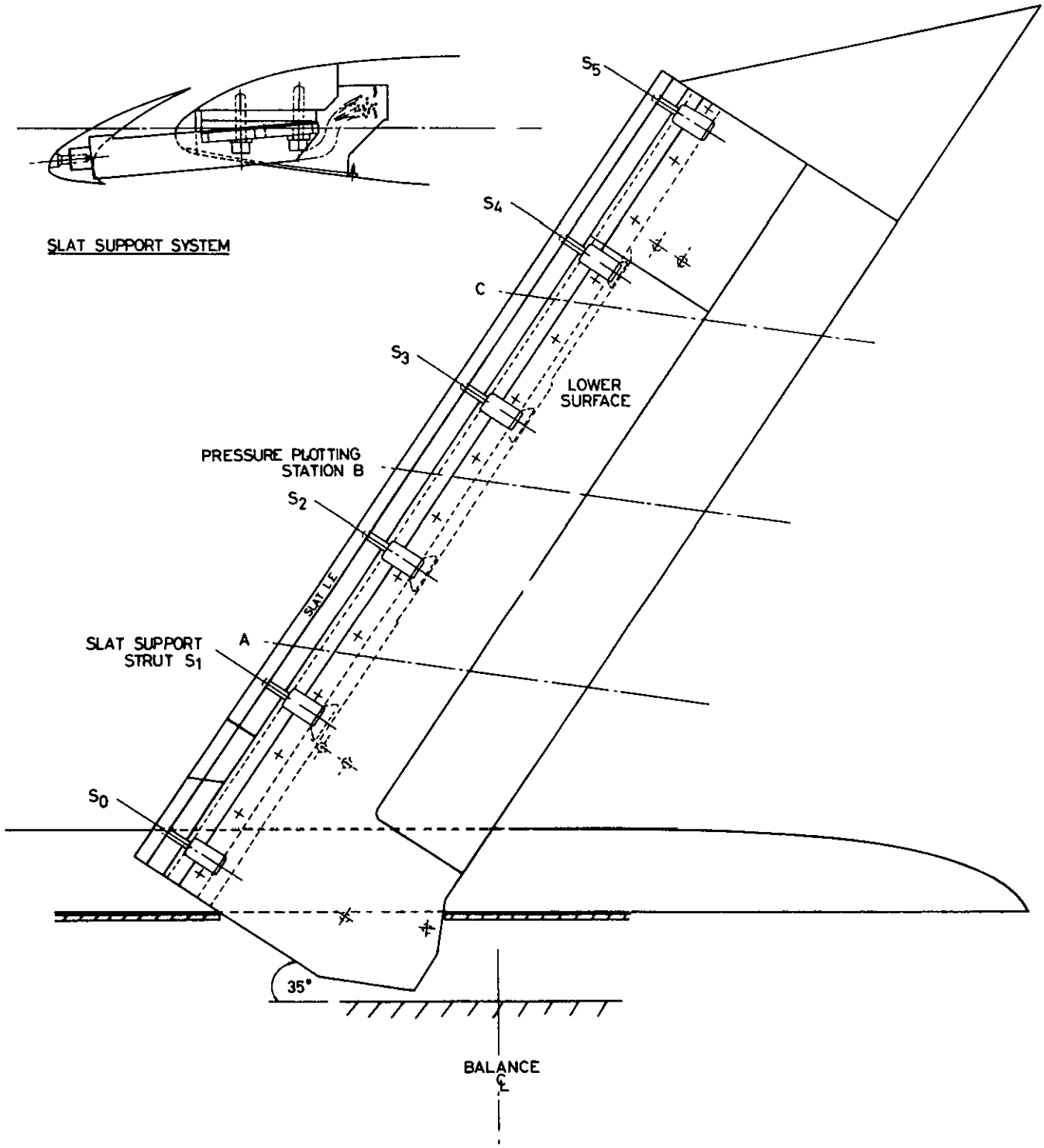

FIG 14 VARIABLE SWEEP WING FOR SLAT/ FLAP RESEARCH

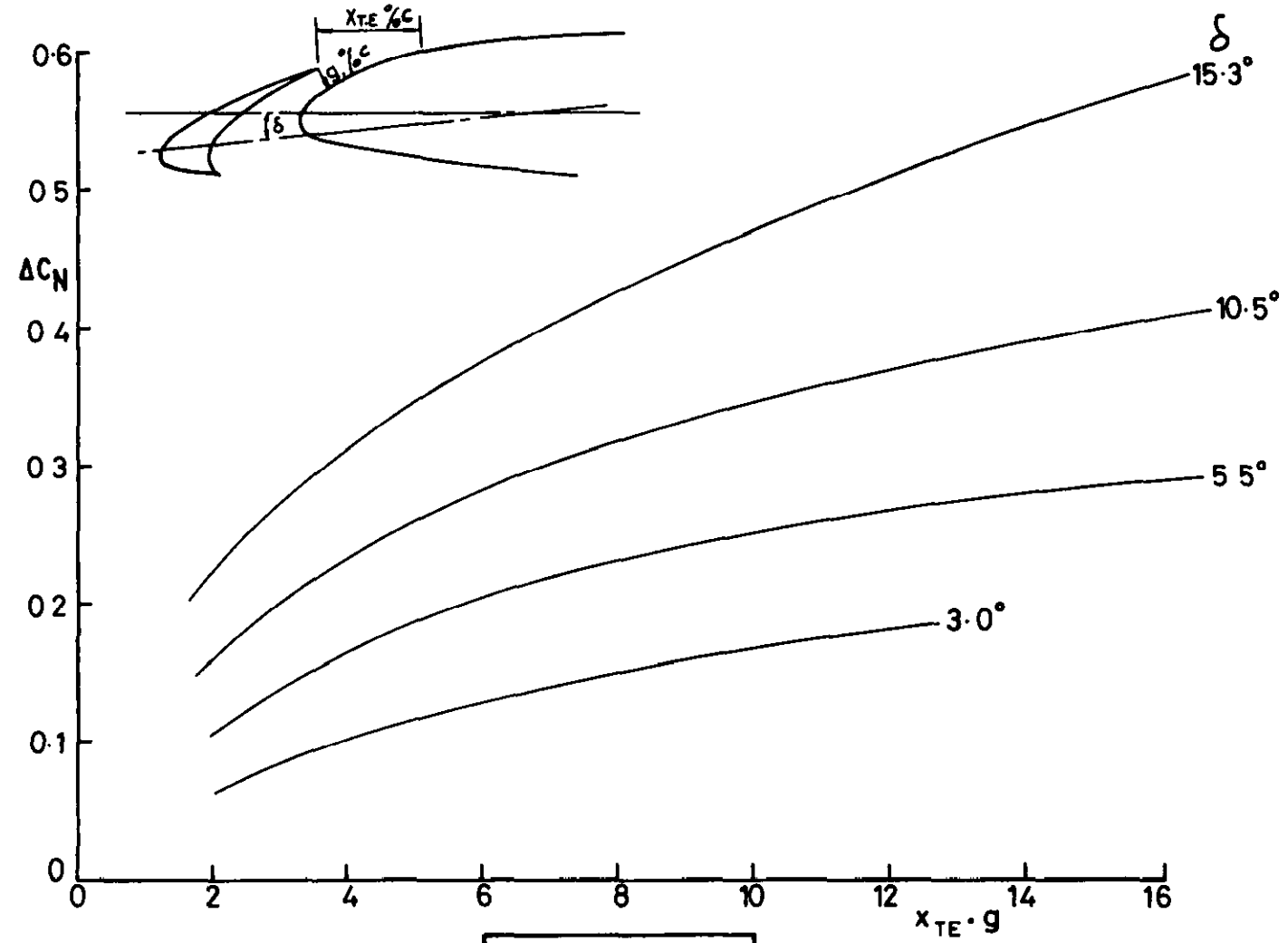

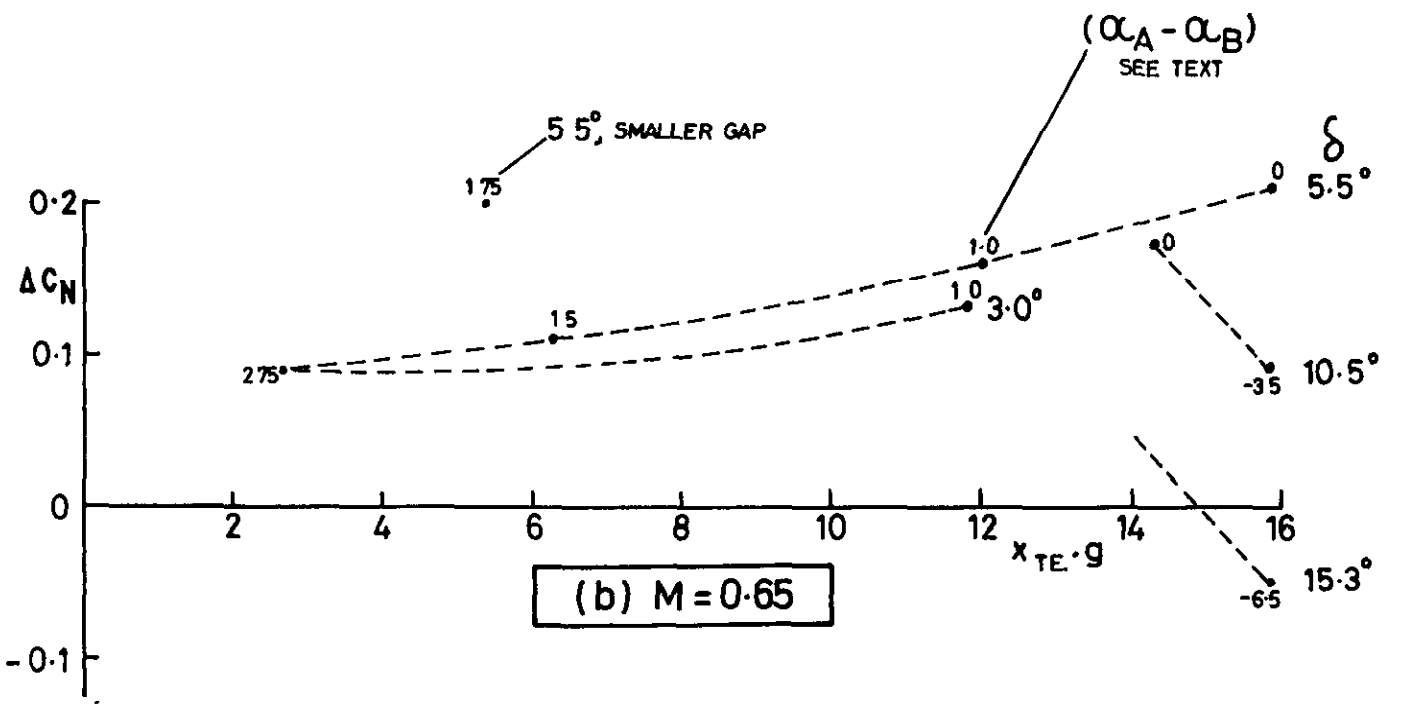

FIG.15 ESTIMATED INCREASE IN USABLE C_N DUE TO SLATS

UNTAPERED WING $\Lambda = 25°$

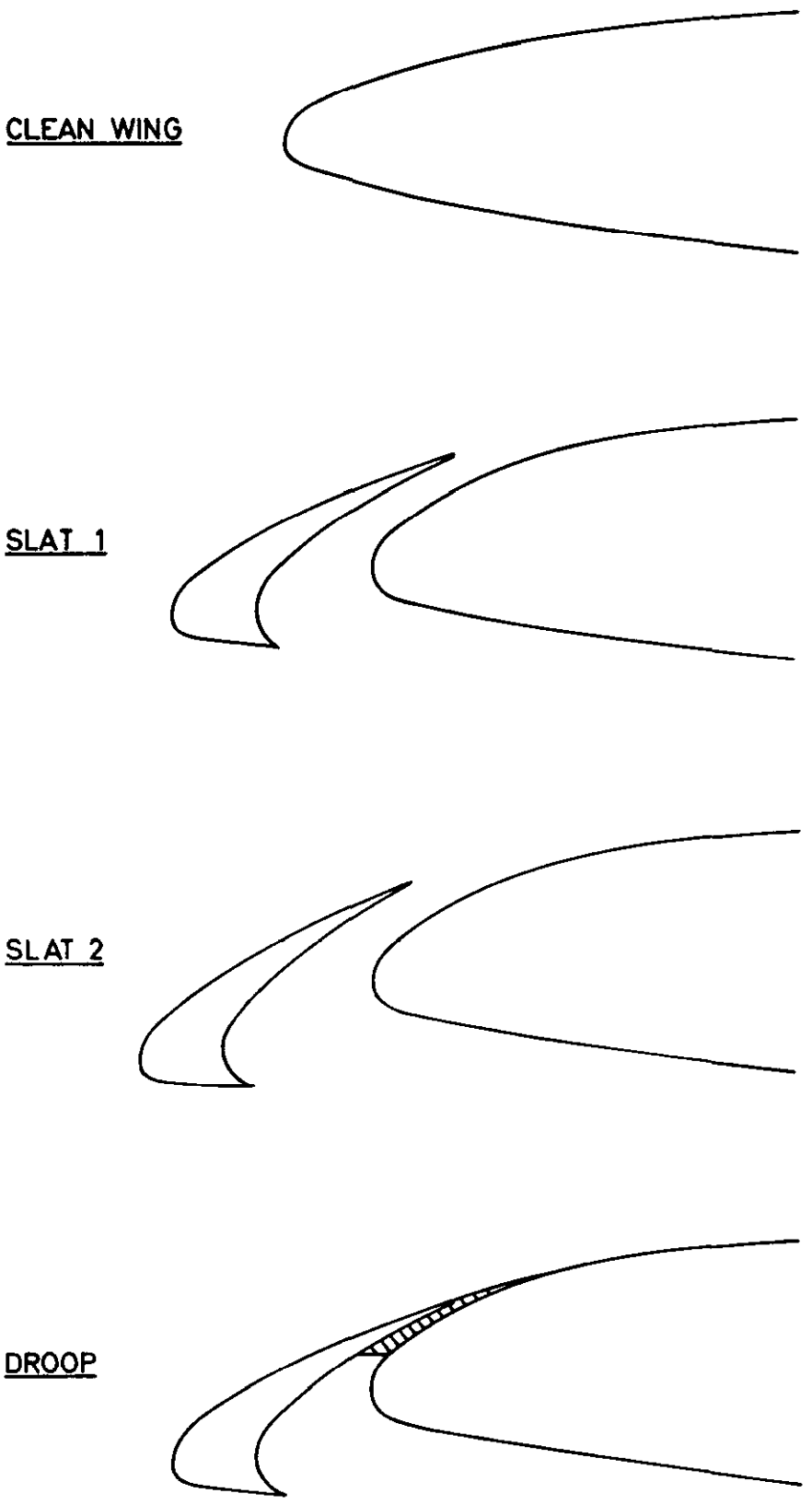

FIG. 16 TYPICAL SLATS TESTED ON RESEARCH WING

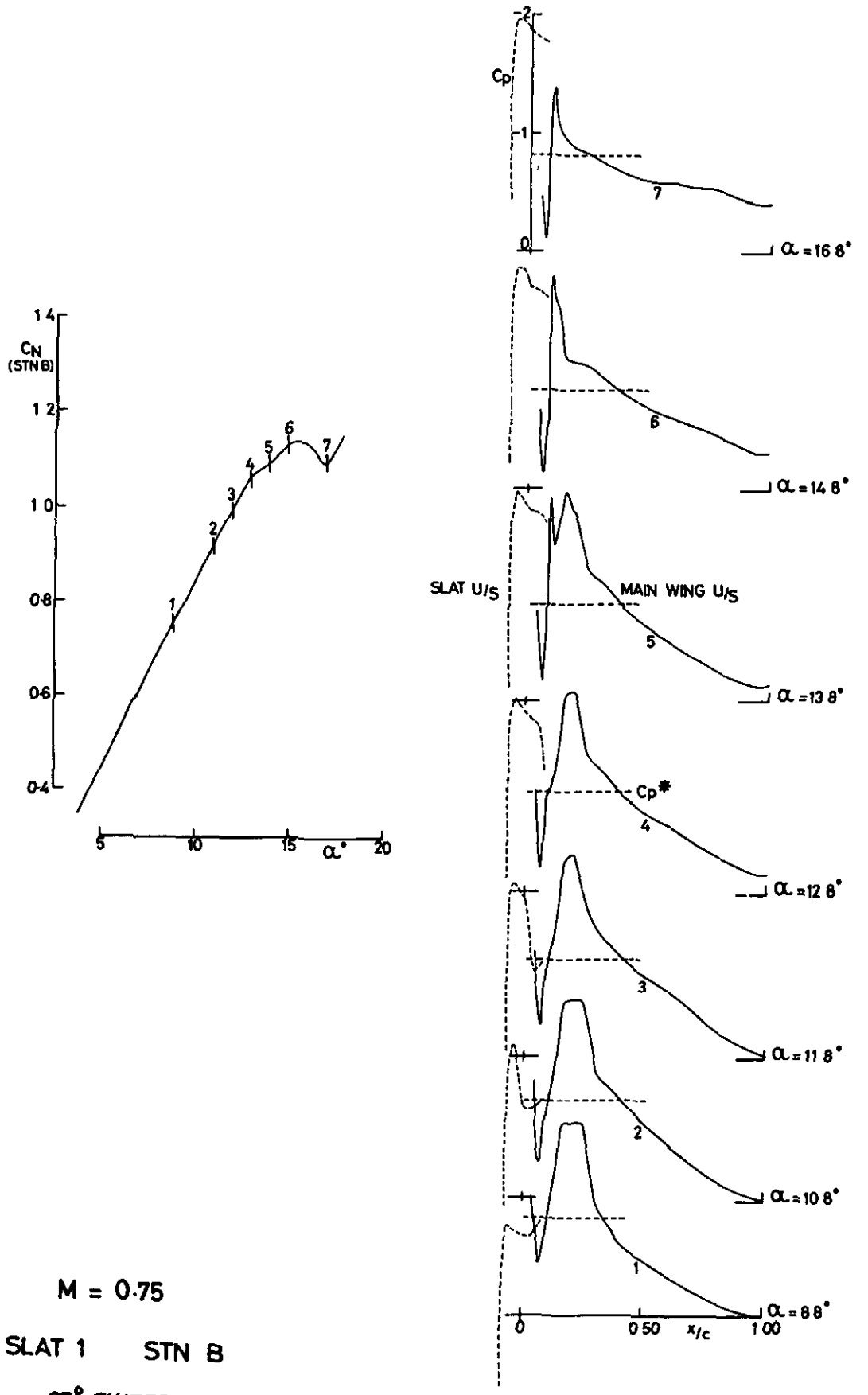

FIG 17 FLOW DEVELOPMENT NEAR MID SEMISPAN WITH TYPICAL SLAT

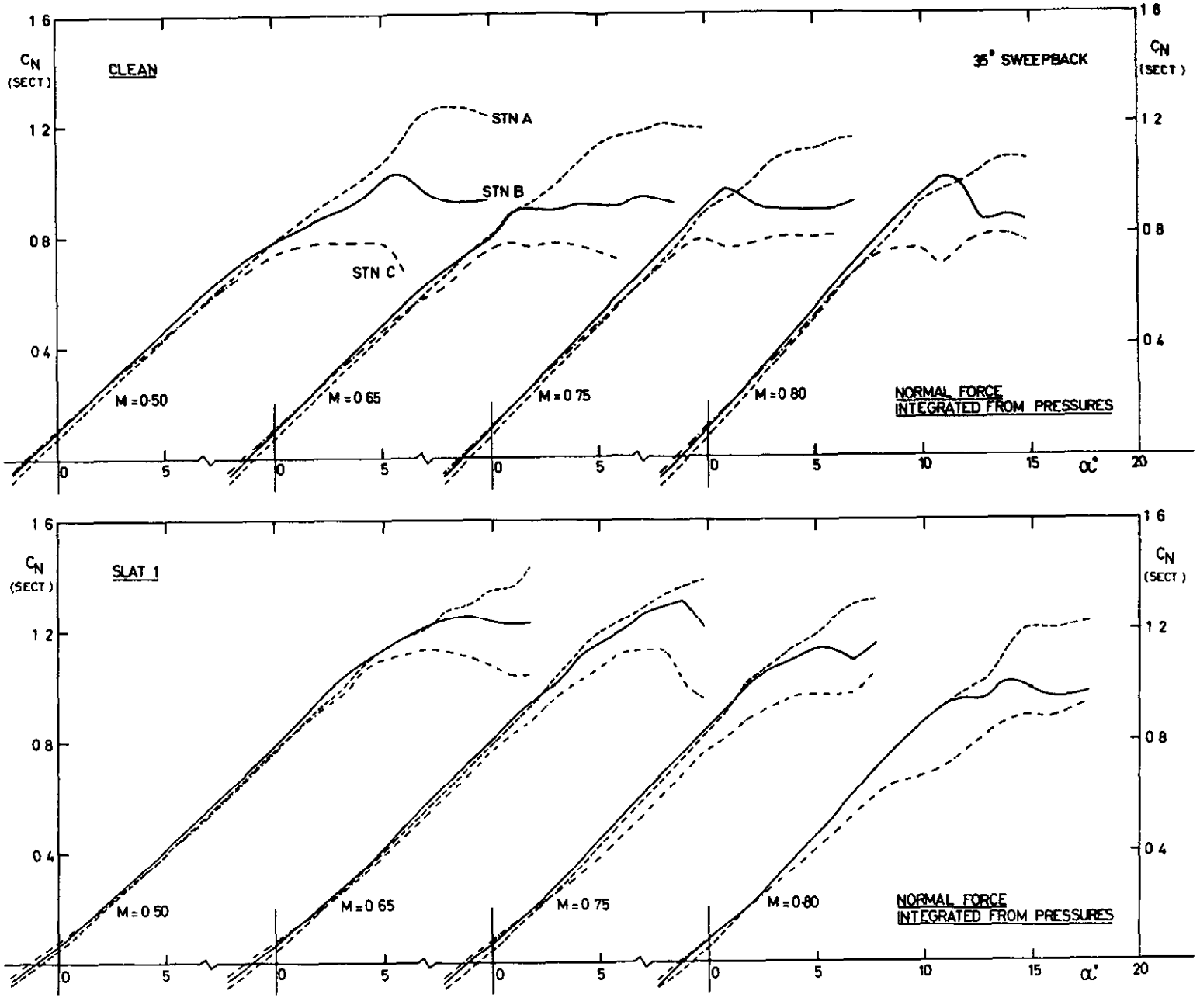

FIG 18 EFFECT OF SLAT ON SPANWISE DEVELOPMENT OF STALL 35° SWEEP

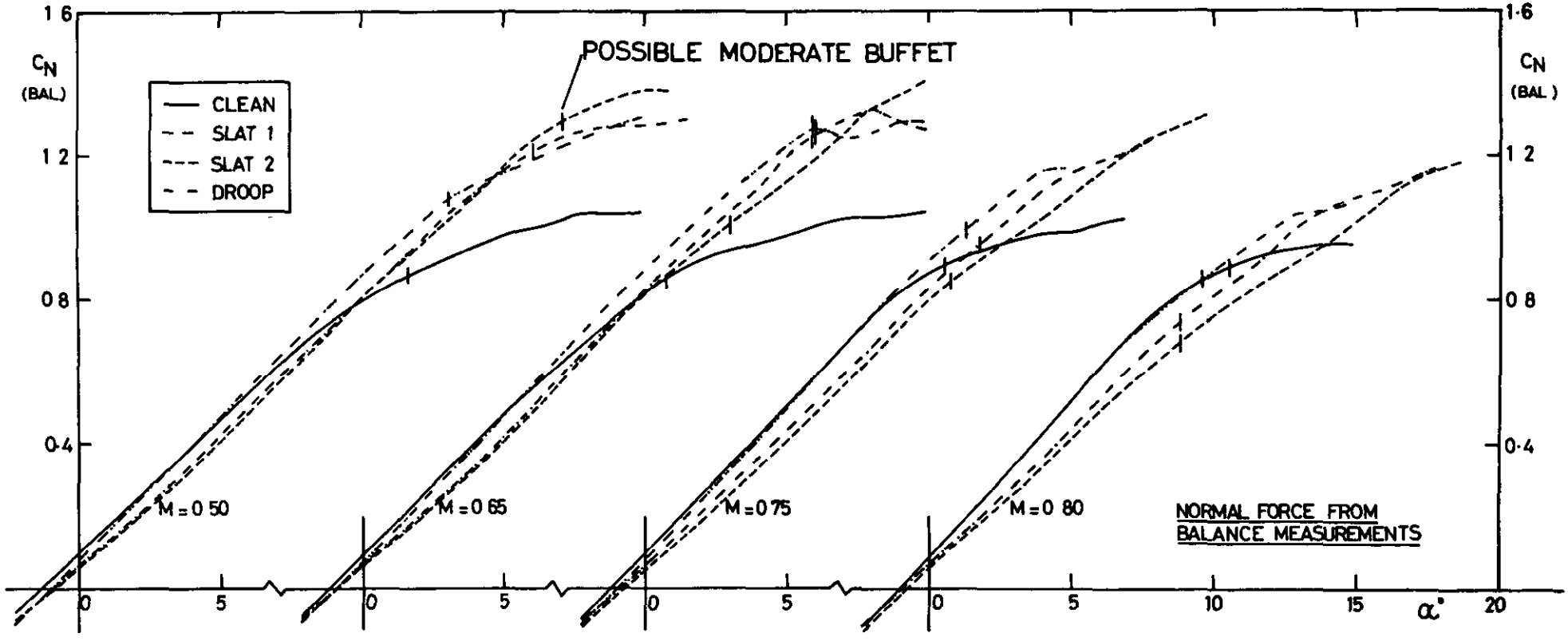

FIG. 19 EFFECT OF SLATS (AND DROOP) ON USABLE LIFT 35° SWEEP

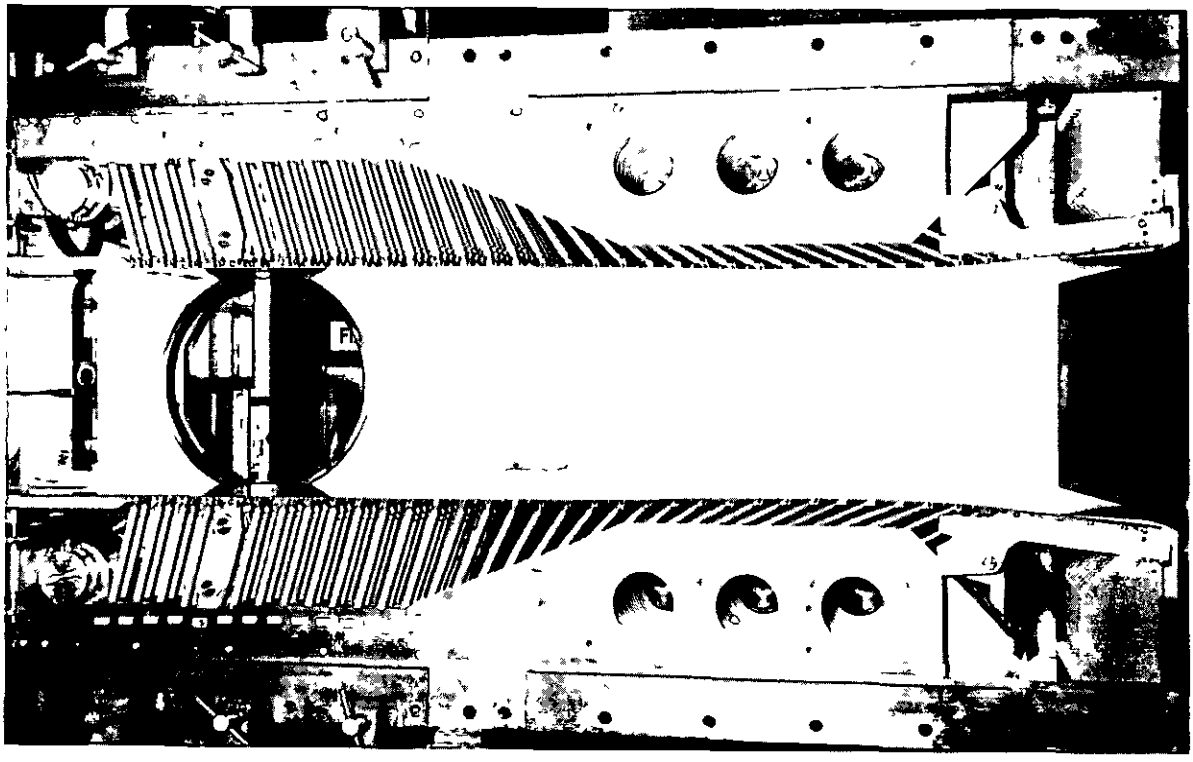

Flexible walls set at shape for $M \leq 1$

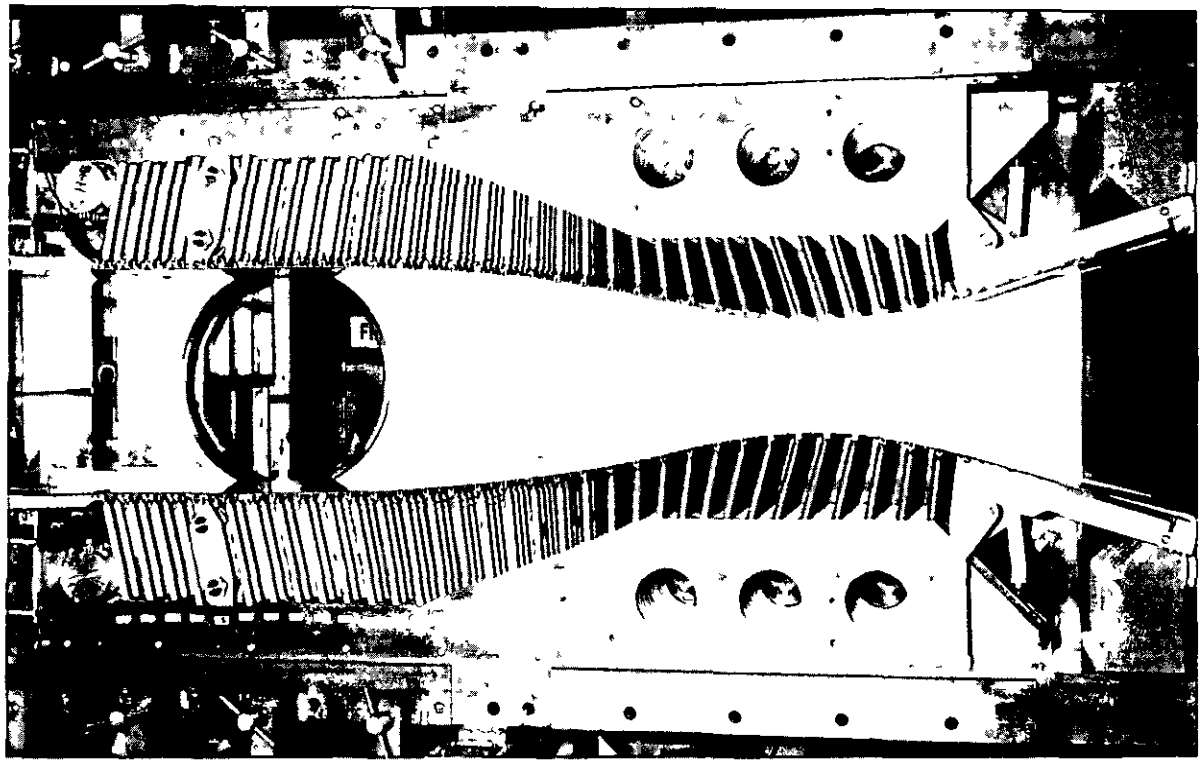

Flexible walls set at shape for $M=2{\cdot}3$

Fig.20 Mechanism used in RAE 18ins x 18ins supersonic tunnel for the rapid and accurate variation of mach number (Based on the RAEVAM principle)

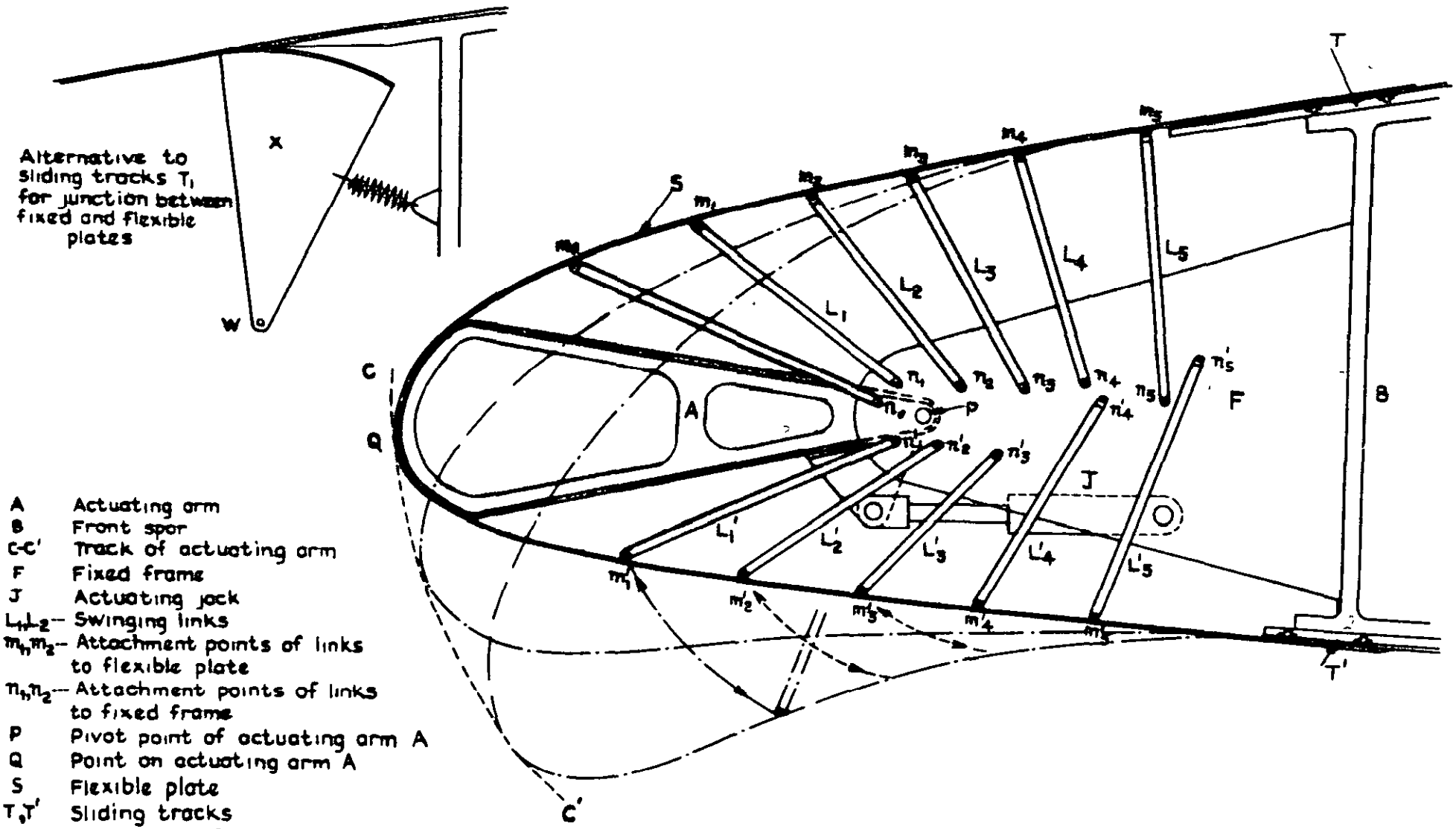

A Actuating arm
B Front spar
C-C' Track of actuating arm
F Fixed frame
J Actuating jack
L_1, L_2 — Swinging links
m_1, m_2 — Attachment points of links to flexible plate
n_1, n_2 — Attachment points of links to fixed frame
P Pivot point of actuating arm A
Q Point on actuating arm A
S Flexible plate
T, T' Sliding tracks
W Pivot point of plate anchorage quadrant X
X Plate anchorage quadrant

Fig. 21 RAEVAM Mechanism for flexible leading-edge section of aerofoil

F' Frame carrying fixed pivot points n_1, n_2—
J Actuating jack for link mechanism
J' Actuating jack for sliding movement
P Pivot point of actuating arm
R Rollers attached to frame F'
T Track for movement of frame F'
C-C' Track of point Q due to jack J
D-D' Track of point Q due to jack J'

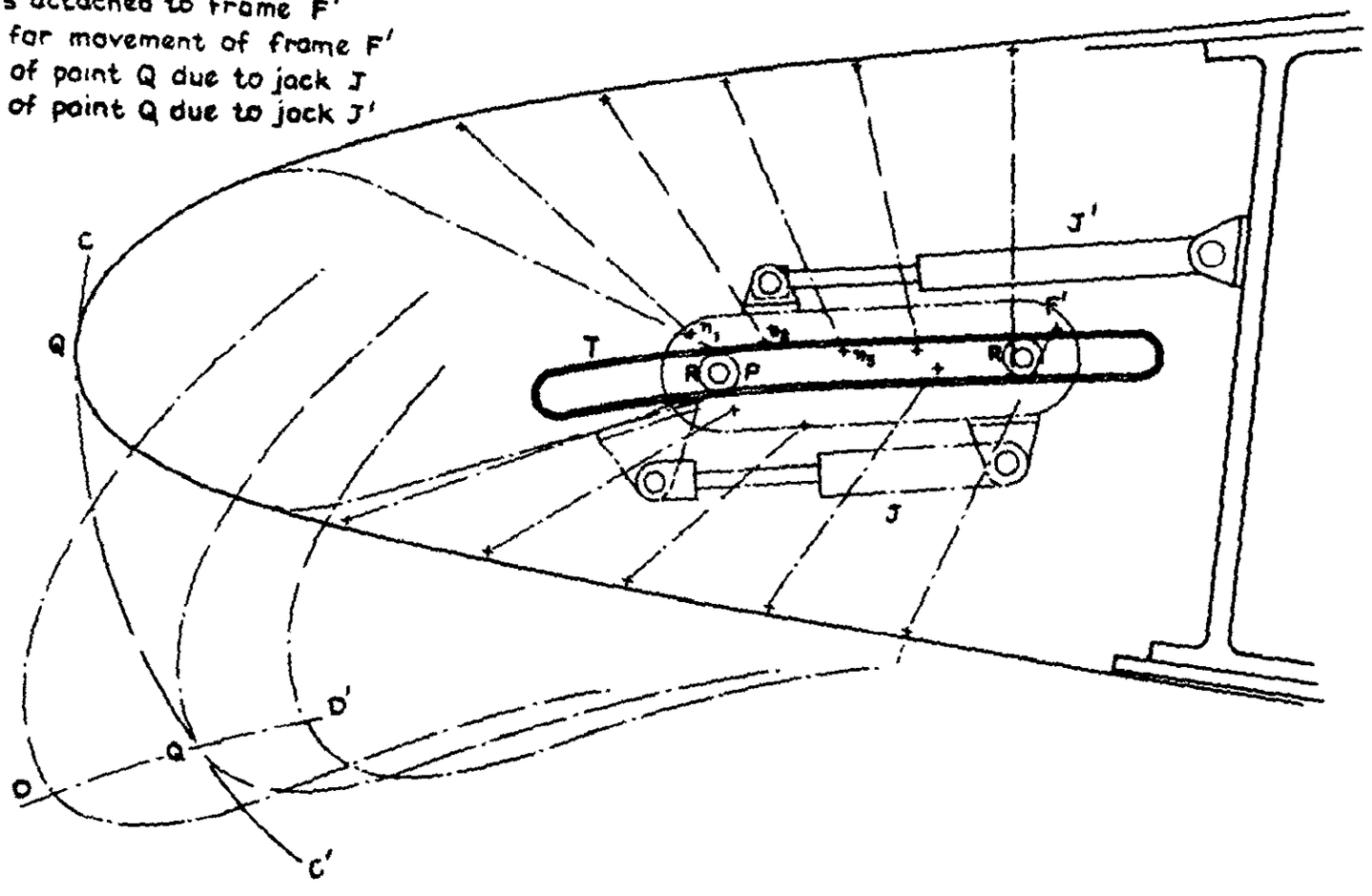

Fig. 22 Combination of flexible nose section with sliding movement

K Frame on which complete nose is mounted
E-E' Track of pivot point P when frame K rotates
U Bearing about which frame K rotates

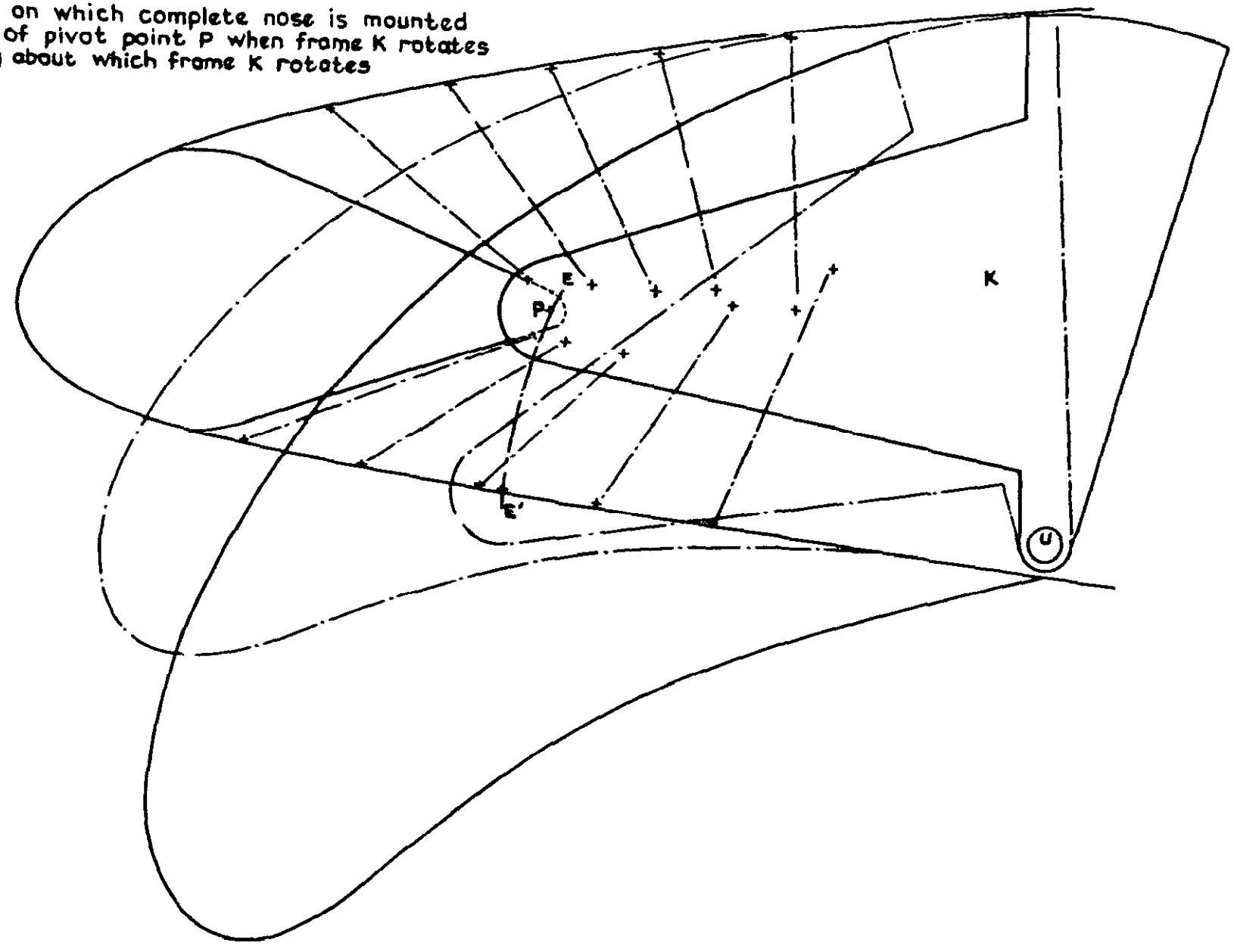

Fig. 23 **Combination of flexible nose section and rotary movement**

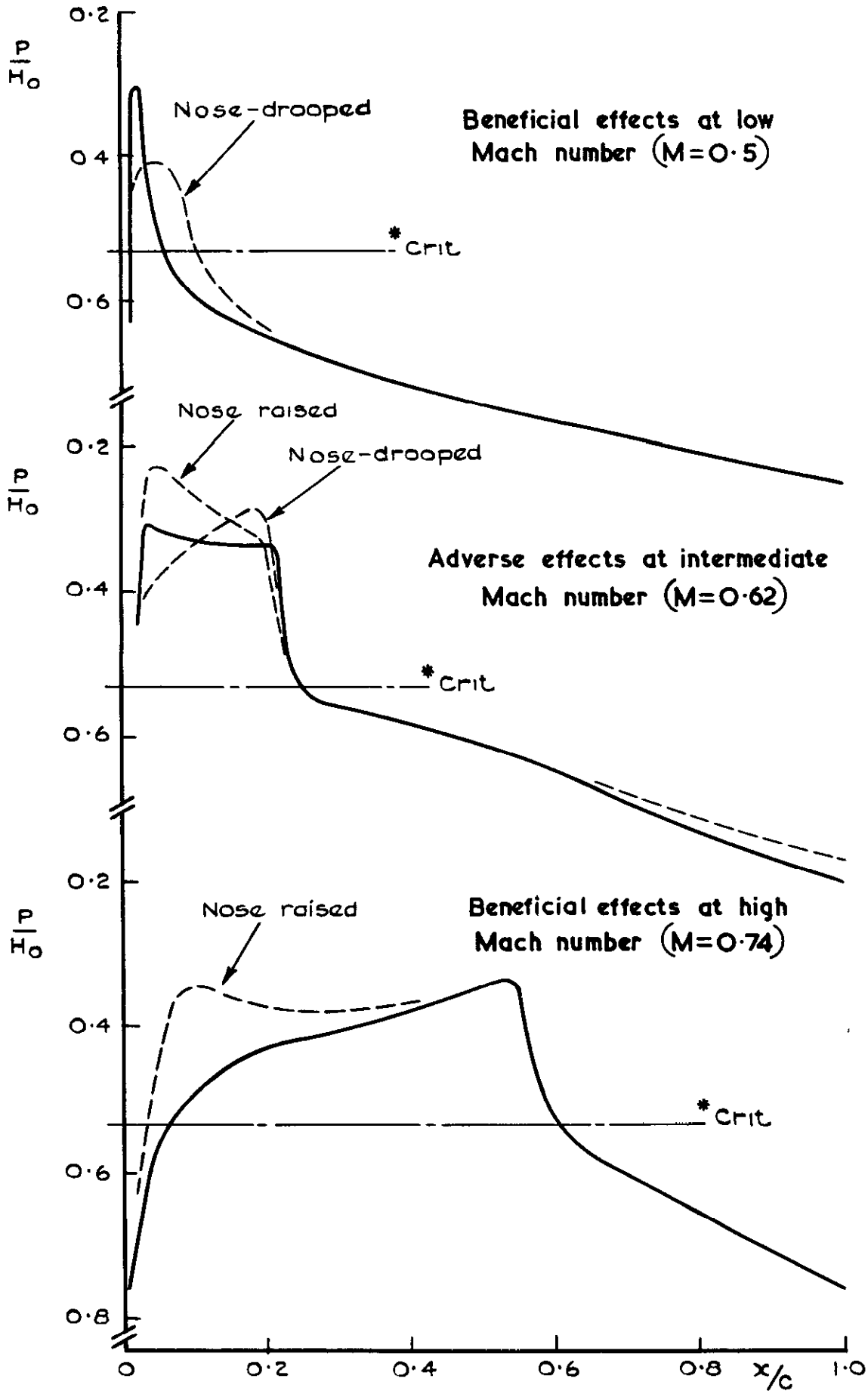

Fig. 24 The diagramatic effects of 'Raevam' deflection of the leading-edge on the basic types of pressure distribution shown in Fig. 1

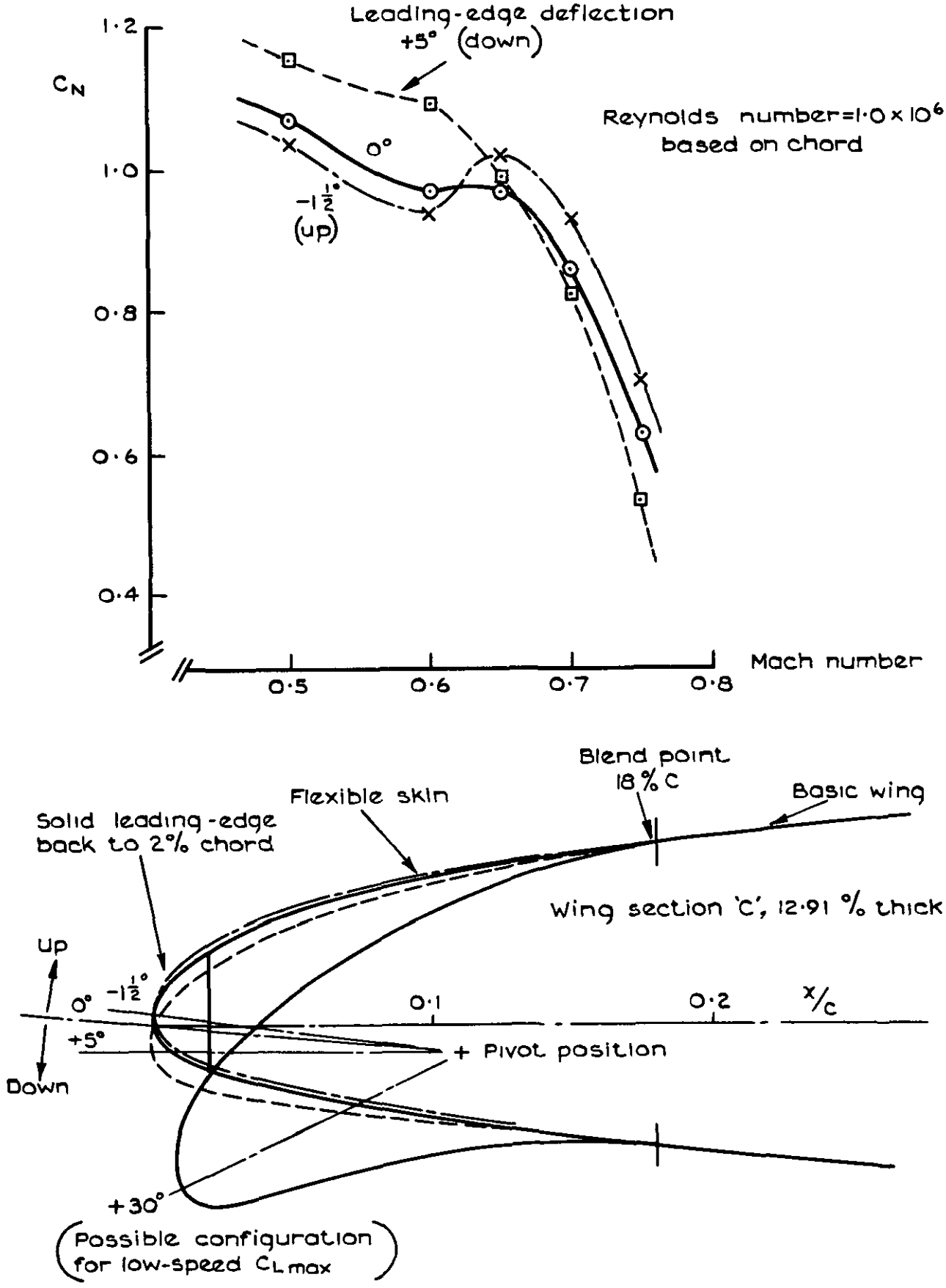

Fig.25 Stall boundary from tunnel tests on a family of nose shapes generated from basic section 'C' using the 'Raevam' device

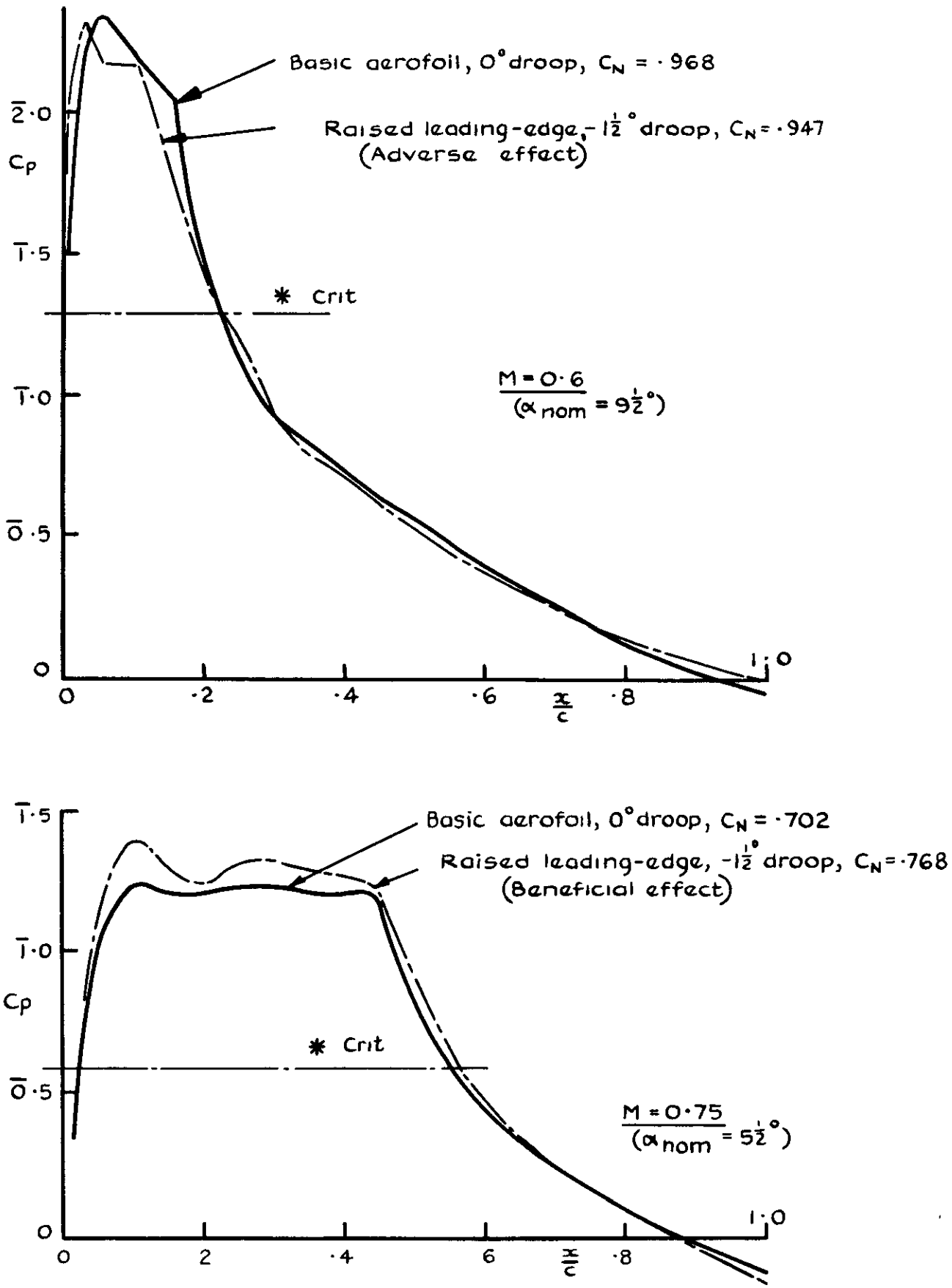

Fig. 26 The effect of Raevam; raising the leading-edge of wing section 'C' at fixed incidence

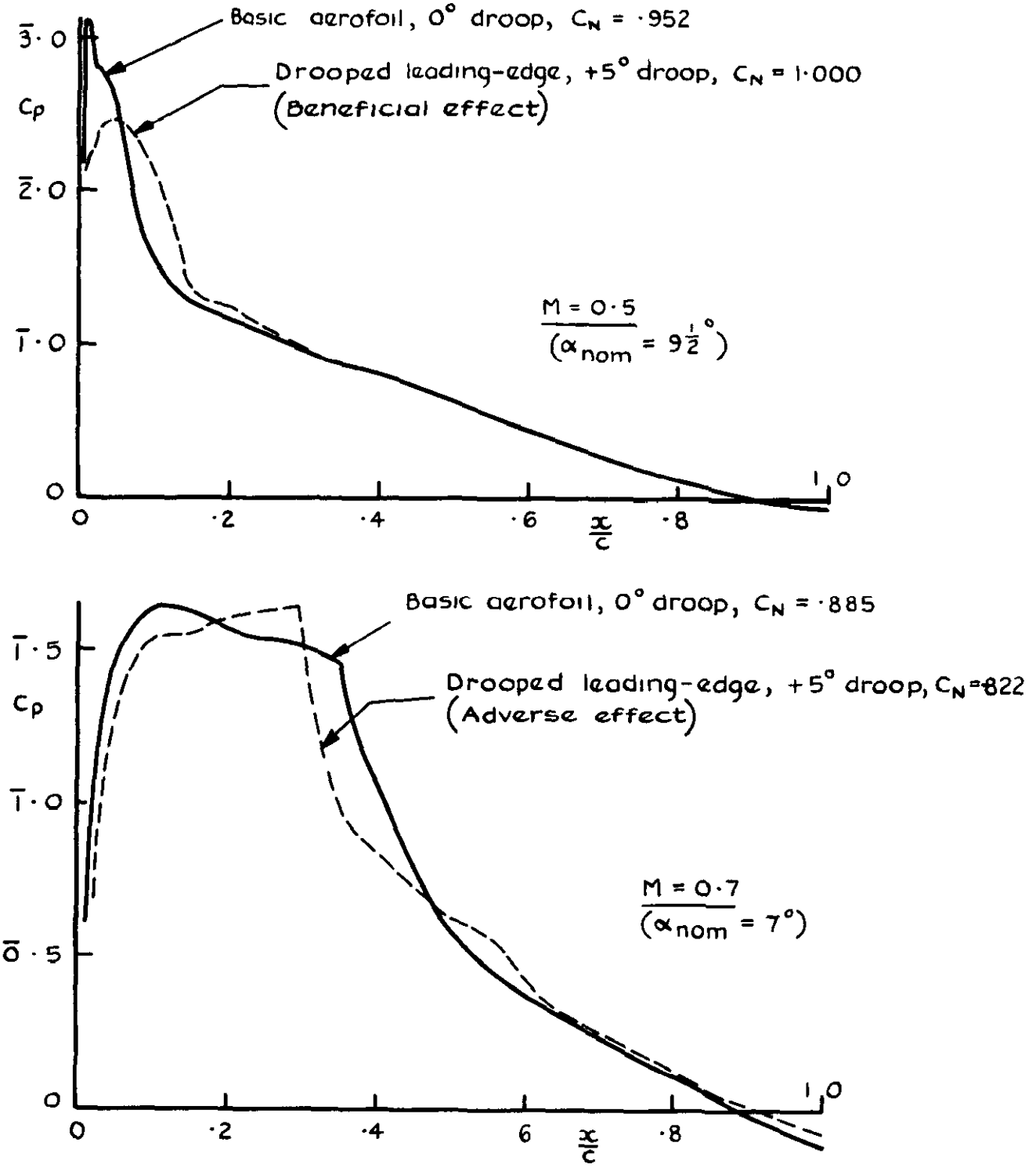

Fig. 27 Effect of Raevam; drooping the leading-edge of wing section 'C' at fixed incidence

Printed in England for Her Majesty's Stationery Office by the Royal Aircraft Establishment, Farnborough Dd 505716 K4 5/73

ARC CP No 1251
May 1972

533 691 1
533 6 013 66
533 6 013.13

Moss, G F
Haines, A. B
Jordan, R

533 694.26
533 691 13

THE EFFECT OF LEADING-EDGE GEOMETRY ON HIGH-SPEED STALLING

In the first part of this paper it is shown by means of an example how small modifications to the leading-edge profile of a sweptwing can result in large effects on lift performance at the stall in the higher range of subsonic speeds The basic types of leading-edge pressure distribution for any one fixed geometry over the whole range of subsonic speed are discussed and the difficulties in designing a profile shape which gives a satisfactory compromise in wing performance across this range is emphasized

In the second part of the paper, two types of variable-geometry device at the leading edge are discussed, each of which allows some degree of optimization in the shape required for good aerodynamic performance across the range of Mach number The first of these, the leading-edge slat, is shown to work in quite a different way at high speeds from that in its

(Over)

These abstract cards are inserted in Technical Reports for the convenience of Librarians and others who need to maintain an Information Index

Cut here

ARC CP No 1251
May 1972

533 691 1
533 6 013 66
533 6 013 13

Moss, G F
Haines, A B
Jordan, R

533 694 26 q
533 691 13

THE EFFECT OF LEADING-EDGE GEOMETRY ON HIGH-SPEED STALLING

In the first part of this paper it is shown by means of an example how small modifications to the leading-edge profile of a sweptwing can result in large effects on lift performance at the stall in the higher range of subsonic speeds The basic types of leading-edge pressure distribution for any one fixed geometry over the whole range of subsonic speed are discussed and the difficulties in designing a profile shape which gives a satisfactory compromise in wing performance across this range is emphasized

In the second part of the paper, two types of variable-geometry device at the leading edge are discussed, each of which allows some degree of optimization in the shape required for good aerodynamic performance across the range of Mach number The first of these, the leading-edge slat, is shown to work in quite a different way at high speeds from that in its

(Over)

Cut here

DETACHABLE ABSTRACT CARDS

DETACHABLE ABSTRACT CARDS

more conventional role at landing and take-off conditions Recent UK research work is used to demonstrate some important aerodynamic features of slats when used at high speeds in near-optimum positions The second type of variable-geometry device is a new one, recently developed within the UK The essential feature is a linkage system, entirely contained within the nose of the profile, which can be used to change the shape of the leading edge of the 'clean' wing in such a way to improve performance over a range of aerodynamic conditions The aerodynamic possibilities of the use of this device in the higher subsonic speed range are demonstrated by reference to some recent UK wind-tunnel tests

more conventional role at landing and take-off conditions Recent UK research work is used to demonstrate some important aerodynamic features of slats when used at high speeds in near-optimum positions The second type of variable-geometry device is a new one, recently developed within the UK The essential feature is a linkage system, entirely contained within the nose of the profile, which can be used to change the shape of the leading edge of the 'clean' wing in such a way to improve performance over a range of aerodynamic conditions The aerodynamic possibilities of the use of this device in the higher subsonic speed range are demonstrated by reference to some recent UK wind-tunnel tests

more conventional role at landing and take-off conditions Recent UK research work is used to demonstrate some important aerodynamic features of slats when used at high speeds in near-optimum positions The second type of variable-geometry device is a new one, recently developed within the UK The essential feature is a linkage system, entirely contained within the nose of the profile, which can be used to change the shape of the leading edge of the 'clean' wing in such a way to improve performance over a range of aerodynamic conditions The aerodynamic possibilities of the use of this device in the higher subsonic speed range are demonstrated by reference to some recent UK wind-tunnel tests

Published by
HER MAJESTY'S STATIONERY OFFICE

To be purchased from
49 High Holborn, London WC1 V 6HB
13a Castle Street, Edinburgh EH2 3AR
109 St Mary Street, Cardiff CF1 1JW
Brazennose Street, Manchester M60 8AS
50 Fairfax Street, Bristol BS1 3DE
258 Broad Street, Birmingham B1 2HE
80 Chichester Street, Belfast BT1 4JY
or through booksellers

C.P. No. 1251

SBN 11 470809 6